The Journal of Experimental Biology 215, 590-604

doi:10.1242/jeb.062869

RESEARCH ARTICLE

Rheb, an activator of target of rapamycin, in the blackback land crab, *Gecarcinus lateralis*: cloning and effects of molting and unweighting on expression in skeletal muscle

Kyle S. MacLea[1], Ali M. Abuhagr[1], Natalie L. Pitts[1], Joseph A. Covi[1,2], Brandon D. Bader[1], Ernest S. Chang[3] and Donald L. Mykles[1,*]

[1]Department of Biology, Colorado State University, Fort Collins, CO 80523, USA, [2]Department of Biology, University of Wisconsin-Stevens Point, Stevens Point, WI 54481, USA and [3]Bodega Marine Laboratory, University of California-Davis, Bodega Bay, CA 94923, USA

*Author for correspondence (don@lamar.colostate.edu)

Accepted 1 November 2011

SUMMARY

Molt-induced claw muscle atrophy in decapod crustaceans facilitates exuviation and is coordinated by ecdysteroid hormones. There is a 4-fold reduction in mass accompanied by remodeling of the contractile apparatus, which is associated with an 11-fold increase in myofibrillar protein synthesis by the end of the premolt period. Loss of a walking limb or claw causes a loss of mass in the associated thoracic musculature; this unweighting atrophy occurs in intermolt and is ecdysteroid independent. Myostatin (Mstn) is a negative regulator of muscle growth in mammals; it suppresses protein synthesis, in part, by inhibiting the insulin/metazoan target of rapamycin (mTOR) signaling pathway. Signaling *via* mTOR activates translation by phosphorylating ribosomal S6 kinase (s6k) and 4E-binding protein 1. Rheb (Ras homolog enriched in brain), a GTP-binding protein, is a key activator of mTOR and is inhibited by Rheb-GTPase-activating protein (GAP). Akt protein kinase inactivates Rheb-GAP, thus slowing Rheb-GTPase activity and maintaining mTOR in the active state. We hypothesized that the large increase in global protein synthesis in claw muscle was due to regulation of mTOR activity by ecdysteroids, caused either directly or indirectly *via* Mstn. In the blackback land crab, *Gecarcinus lateralis*, a Mstn-like gene (*Gl-Mstn*) is downregulated as much as 17-fold in claw muscle during premolt and upregulated 3-fold in unweighted thoracic muscle during intermolt. *Gl-Mstn* expression in claw muscle is negatively correlated with hemolymph ecdysteroid level. Full-length cDNAs encoding Rheb orthologs from three crustacean species (*G. lateralis*, *Carcinus maenas* and *Homarus americanus*), as well as partial cDNAs encoding Akt (*Gl-Akt*), mTOR (*Gl-mTOR*) and s6k (*Gl-s6k*) from *G. lateralis*, were cloned. The effects of molting on insulin/mTOR signaling components were quantified in claw closer, weighted thoracic and unweighted thoracic muscles using quantitative polymerase chain reaction. *Gl-Rheb* mRNA levels increased 3.4-fold and 3.9-fold during premolt in claw muscles from animals induced to molt by eyestalk ablation (ESA) and multiple leg autotomy (MLA), respectively, and mRNA levels were positively correlated with hemolymph ecdysteroids. There was little or no effect of molting on *Gl-Rheb* expression in weighted thoracic muscle and no correlation of *Gl-Rheb* mRNA with ecdysteroid titer. There were significant changes in *Gl-Akt*, *Gl-mTOR* and *Gl-s6k* expression with molt stage. These changes were transient and were not correlated with hemolymph ecdysteroids. The two muscles differed in terms of the relationship between *Gl-Rheb* and *Gl-Mstn* expression. In thoracic muscle, *Gl-Rheb* mRNA was positively correlated with *Gl-Mstn* mRNA in both ESA and MLA animals. By contrast, *Gl-Rheb* mRNA in claw muscle was negatively correlated with *Gl-Mstn* mRNA in ESA animals, and no correlation was observed in MLA animals. Unweighting increased *Gl-Rheb* expression in thoracic muscle at all molt stages; the greatest difference (2.2-fold) was observed in intermolt animals. There was also a 1.3-fold increase in *Gl-s6k* mRNA level in unweighted thoracic muscle. These data indicate that the mTOR pathway is upregulated in atrophic muscles. *Gl-Rheb*, in particular, appears to play a role in the molt-induced increase in protein synthesis in the claw muscle.

Key words: myostatin, mTOR, target of rapamycin, Rheb, Akt, S6 kinase, gene expression, Crustacea, Arthropoda, ecdysteroid, molting, mRNA, skeletal muscle, eyestalk ablation, tissue distribution, cDNA cloning, DNA sequence, amino acid sequence, K-box.

INTRODUCTION

Skeletal muscle is a plastic tissue that responds to a variety of physiological conditions. In mammals, nutrition, steroid hormones, innervation, stretch, exercise and disease alter fiber size (reviewed by Cardozo et al., 2010; Drummond et al., 2009a; Favier et al., 2008; Matsakas and Patel, 2009b; Zhang et al., 2007). Mammalian muscle atrophies in response to aging, denervation, glucocorticoids, unloading, sepsis and cancer cachexia (reviewed by Frost and Lang, 2011; Furlow et al., 2010; Glass, 2010; Schakman et al., 2009; Urso, 2009). In decapod crustaceans, two types of muscle atrophy are documented: (1) a molt-induced claw muscle atrophy in response to molting hormone (ecdysteroids), which allows easier passage of the claw through the small basi-ischial joint when the old exoskeleton is shed at ecdysis (reviewed by Mykles, 1997; Mykles, 1999; Mykles and Skinner, 1982a); and (2) an unweighting atrophy of the thoracic muscles in response to autotomy, or voluntary loss, of the associated limb (Griffis et al., 2001; Moffett, 1987; Schmiege et al., 1992). Unlike claw muscle

atrophy, thoracic muscle atrophy can occur during the intermolt period when hemolymph ecdysteroid levels are low (Mykles, 2011). Claw muscle atrophy coincides with an extensive remodeling of the contractile apparatus, resulting from the preferential loss of thin filaments (Ismail and Mykles, 1992; Mykles and Skinner, 1981; Mykles and Skinner, 1982b). It is thought that the remaining thick filaments provide a framework for the incorporation of thin filaments into the sarcomere during the post-molt period (Mykles and Skinner, 1981). An accelerated protein turnover, resulting from an increase in protein synthesis, occurs during premolt and is hypothesized to facilitate the exchange of myofilaments between soluble and myofibrillar protein pools required for remodeling (Mykles, 1997).

Myostatin (Mstn) is an autocrine/paracrine factor that inhibits muscle growth in vertebrates (reviewed by Glass, 2010; McCarthy and Esser, 2010; Rodgers and Garikipati, 2008; Stinckens et al., 2011). It acts by suppressing protein synthesis at the same time as it increases protein degradation, resulting in a reduction of skeletal muscle mass (reviewed by Matsakas and Patel, 2009a; McCarthy and Esser, 2010; Tisdale, 2009; Zhang et al., 2007). Mstn may also regulate muscle growth in invertebrates. cDNAs encoding Mstn-like proteins have been characterized in mollusks and arthropods (Covi et al., 2008; De Santis et al., 2011; Hu et al., 2010; Kim et al., 2004; Kim et al., 2009; Kim et al., 2010; Lo and Frasch, 1999; MacLea et al., 2010). In blackback land crabs (*Gecarcinus lateralis*), molt-induced atrophy and unweighting atrophy have opposite effects on *Gl-Mstn* expression in claw closer and thoracic muscles, respectively. Unweighting increases *Gl-Mstn* mRNA levels 3-fold in thoracic muscles in intermolt animals (Covi et al., 2010). By contrast, *Gl-Mstn* mRNA levels in claw muscle decrease ~17-fold as protein synthesis of myofibrillar and soluble proteins increase 11-fold and 13- fold, respectively, during premolt (Covi et al., 2010). *Gl-Mstn* mRNA level in weighted thoracic muscle decreases only ~5-fold (Covi et al., 2010). In the American lobster, *Homarus americanus*, *Ha-Mstn* expression in claw closer muscles over the course of the molt cycle varies in very similar ways to that observed in *G. lateralis*, underscoring the conservation of the transcriptional regulatory mechanism among decapod crustaceans (MacLea et al., 2010).

In mammals, Mstn represses protein synthesis by inhibiting the metazoan target of rapamycin (mTOR) (reviewed by Drummond et al., 2009a; Glass, 2010; Matsakas and Patel, 2009a; McCarthy and Esser, 2010; Otto and Patel, 2010). mTOR is a serine/theonine protein kinase that associates with Rheb (Ras homolog enriched in brain), Raptor and GβL to form the mTOR Complex 1 (mTORC1) (reviewed by Proud, 2009; Wullschleger et al., 2006). mTORC1 is a downstream target of the insulin/PI_3 kinase/Akt signaling pathway and stimulates protein synthesis at the translational level by phosphorylating ribosomal S6 kinase (s6k) and 4E-binding protein 1 (Proud, 2009; Wullschleger et al., 2006). Binding of GTP to Rheb activates mTORC1 while hydrolysis of GTP to GDP, which is stimulated by Rheb-GAP [tuberous sclerosis complex 1 and 2 (TSC1/2)], inactivates mTORC1 (Aspuria and Tamanoi, 2004; Wullschleger et al., 2006). Akt inactivates Rheb-GAP, thus maintaining mTORC1 in the activated state by inhibiting GTP hydrolysis. Mstn signaling inhibits mTOR *via* Akt in mammalian skeletal muscles (Amirouche et al., 2009; Trendelenburg et al., 2009). Mstn downregulation stimulates protein synthesis and Akt and s6k phosphorylation (Lipina et al., 2010; Morissette et al., 2009; Welle et al., 2009; Welle et al., 2011). These data indicate that there is cross-talk between Mstn and mTOR signaling pathways in mammalian skeletal muscles.

Ecdysteroid regulation of protein synthesis in crustacean muscle is primarily at the translational level. Elevated ecdysteroid levels have little effect on actin and myosin heavy chain mRNA levels (El Haj, 1999; Medler et al., 2005; Whiteley and El Haj, 1997). Increased protein synthesis during premolt is correlated with increased ribosomal activity (El Haj et al., 1996; Skinner, 1965; Skinner, 1968). Autoradiographic analysis of soluble and myofibrillar proteins shows that the large increase in protein synthesis in atrophic claw muscle is consistent with enhanced translation of existing mRNA into protein (Covi et al., 2010). Crustacean Mstn, like mammalian Mstn, may suppress translation by inhibiting insulin/mTOR signaling. A potential target is Rheb, a member of the Ras superfamily of GTP-binding proteins (reviewed by Reuther and Der, 2000). Rheb is a crucial upstream activator of mTOR (Aspuria and Tamanoi, 2004; Frost and Lang, 2011; Li et al., 2004; Manning and Cantley, 2003). Overexpression of Rheb stimulates cell growth while knockdown of Rheb expression inhibits protein synthesis and cell growth in insects (Hall et al., 2007; Patel et al., 2003) [see additional references in Aspuria and Tamanoi (Aspuria and Tamanoi, 2004)].

The purpose of this study was to determine the effects of molt induction and unweighting on the expression of insulin/mTOR signaling components in *G. lateralis* claw closer and thoracic muscles, as well as to determine if the expression of *Gl-Mstn* is coupled to the expression of *Gl-Rheb* or other components of the insulin/mTOR signaling pathway. Our knowledge of the insulin/mTOR pathway in crustaceans and its role in development and growth is fragmentary at best. Insulin-like peptides have been isolated from crustacean tissues (Gallardo et al., 2003; Hatt et al., 1997) and the androgenic gland expresses an insulin-like growth factor that determines male development (Banzai et al., 2011; Manor et al., 2007; Rosen et al., 2010; Sroyraya et al., 2010; Ventura et al., 2009). Insulin receptor tyrosine kinases and phosphotyrosyl phosphatases are present in crustacean tissues (Chuang and Wang, 1993; Chuang and Wang, 1994; Kucharski et al., 1999; Kucharski et al., 2002; Lin et al., 1993). In the present study, we report the characterization of cDNAs encoding Rheb, Akt, mTOR and s6k from *G. lateralis* and Rheb from the green shore crab (*Carcinus maenas*) and *H. americanus*. Quantitative polymerase chain reaction (qPCR) was used to quantify the expression of *Gl-Rheb*, *Gl-mTOR*, *Gl-Akt* and *Gl-s6k* in claw closer, weighted thoracic and unweighted thoracic muscles. Molting was induced by eyestalk ablation (ESA) and multiple leg autotomy (MLA). cDNA from a previous study (Covi et al., 2010) was used to directly compare the expression of mTOR signaling components with *Gl-Mstn* expression and hemolymph ecdysteroid level.

MATERIALS AND METHODS

Animals and experimental treatments

Adult male blackback land crabs (*Gecarcinus lateralis* Fréminville 1835) were shipped to Colorado, USA, from the Dominican Republic and maintained as described (Covi et al., 2010). Molting was induced by either MLA or ESA (for reviews, see Mykles, 2001; Skinner, 1985). Progression of animals through the premolt period for both methods was monitored by measuring the length of a limb regenerate at the position of the third walking leg, called the regeneration (R) index (R=length of regenerate×100/carapace width) (Holland and Skinner, 1976; Yu et al., 2002). For MLA animals, all eight walking legs were autotomized. For ESA animals, one walking leg was autotomized and a basal regenerate was allowed to form prior to ESA. One claw was also autotomized from intact and MLA animals to determine the effects of unweighting; weighted

muscles were harvested from the thoracic segment with a claw, and unweighted muscles were harvested from the thoracic segment without a claw from the same animal.

Intermolt adult green shore crab, *Carcinus maenas* Linnaeus 1758, and American lobster, *Homarus americanus* H. Milne-Edwards 1837, were obtained from Bodega Marine Laboratory, Bodega Bay, CA, USA (MacLea et al., 2010; McDonald et al., 2011).

Cloning of cDNAs encoding Rheb, mTOR, s6k and Akt

Reverse transcriptase-polymerase chain reaction (RT-PCR) and rapid amplification of cDNA ends (RACE) were used to clone the cDNAs encoding *Gl-Rheb*, *Gl-mTOR*, *Gl-Akt* and *Gl-s6k*. RNA isolation from *G. lateralis* skeletal muscles and cDNA synthesis were the same as described in Covi et al. (Covi et al., 2010). PCR used 0.5 µl of the first-strand cDNA as a template and forward and reverse primers (10 pmol each; Table 1) synthesized by Integrated DNA Technology (IDT; Coralville, IA, USA). For the cloning of *Gl-Rheb*, specific primers directed against the *Cm-Rheb* expressed sequence tag (EST) sequence (GenBank #HM989970) were used (see below). For all other genes degenerate primers were designed using iCODEHOP (Boyce et al., 2009) or by hand using a multiple sequence alignment of various homologous proteins and a codon chart to target areas of high conservation in protein sequences from other arthropod sequences.

Cm-Rheb (GenBank #HM989970) and *Ha-Rheb* (#HM989972) were cloned from *C. maenas* or *H. americanus* cDNA, respectively, on the basis of sequences determined by multiple sequence alignment of several EST clones provided by the Mount Desert

Table 1. Oligonucleotide primers used in the cloning or expression analysis of mTOR signaling components from *Gecarcinus lateralis* (Gl), *Carcinus maenas* (Cm) or *Homarus americanus* (Ha)

Primer temperature (ºC)	Sequence (5′–3′)	Application(s)	Annealing
Ha-EF2 F1	TTCTATGCCTTCGGACGTGTGTTCTC	E	62
Ha-EF2 R1	TGATGGTGCCAGTCTTGACCAGGTAC	E	62
Ha-Rheb F1	TTTGTGGACAGTTATGATCC	E	62
Ha-Rheb R1	AAGATGCTGTATTCATCTTGTCC	E	62
Cm RT EF2 FWD1	CCATCAAGAGCTCCGACAATGAGCG	E	62
Cm RT EF2 REV1	CATTTCGGCACGGTACTTCTGAGCG	E	62
Cm-Rheb F1	ATGGGCAAAGTCACAGTTCC	E	62
Cm-Rheb R1	GTCAGGAAGATGGTGGCAAT	E	62
Gl cEF2 F1	TTCTATGCCTTTGGCCGTGTCTTCTC	E	62
Gl cEF2 R1	TGATGGTGCCCGTCTTAACCAGATAC	E	62
Gl-Rheb qPCR F1	TTTGTGGACAGCTATGATCCC	E	62
Gl-Rheb qPCR R1	AAGATGCTATACTCATCCTGACC	E	62
Gl-mTOR qPCR F2	AGAAGATCCTGCTGAACATCGAG	E	62
Gl-mTOR qPCR R2	AGGAGGGACTCTTGAACCACAG	E	62
Gl-Akt qPCR F2	AACTCAAGTACTCCAGCGATGATG	E	62
Gl-Akt qPCR R1	GGTTGCTACTCTTTTCACGACAGA	E	62
Gl-s6k qPCR F2	GGACATGTGAAGCTCACAGACTTT	E	62
Gl-s6k qPCR R1	TTCCCCTTCAGGATCTTCTCTATG	E	62
Gl-mTOR degF	CCGCCAGTTCAGCARNGGRTCRTA	I	53
Gl-mTOR degR	GCAGGACGAGCGGBTNATGSARYT	I	53
Gl-mTOR F1	TGCTGTGGTTCAAGAGTCCCT	3′ (outer)	58
Gl-mTOR F2	GCAAGATCATCCACATCGACTT	3′ (inner)	55
Gl-Akt degF2	TGAACAACTTCACCGTGAARCARTGYCA	I	51
Gl-Akt degR1	TCGCCGCCGTTCACRTAYTCCAT	I	51
Gl-Akt F1-1	TGTCGTGAAAAGAGTAGCAACCAT	3′ (outer)	56
Gl-Akt F2-1	CCTCAAGTATTCCTTCCAAACCAA	3′ (inner)	55
Gl-Akt F1-2	TTGCACTGGGTTACTTACACGAA	3′ (outer)	56
Gl-Akt F2-2	GAAGACATCTCCTACGGCTCAA	3′ (inner)	56
Gl-Akt R1	CTGGAGTACTTGAGTTGGATGTGC	5′ (outer)	57
Gl-Akt R2	TTCCATCCATTCTTCCCTGTCACT	5′ (inner)	57
Gl-s6k degF2	TCGTGGACCTGGTGTAYGCNTTYCA	I	50
Gl-s6k degR1	TCTGCTTGGTGAACTTGSWRTCRAAYTG	I	50
Gl-s6k F1	AACCTTCCACCCTACCTGACT	3′ (outer)	57
Gl-s6k F2	GTGGTGATGATGATGTGAGCCAAT	3′ (inner)	57
Gl-s6k R1	TGATGCCCTCAGAGTGAAGATGTT	5’ (outer)	58
Gl-s6k R2	CAGGATGAGATATAGCTTACC	5′ (inner)	51
Gl-Rheb degF1	ATGCCTCCMAARGAYAG	I (outer)	45
Gl-Rheb degF2	AAAGTRGCCGTWATGGGC	I (inner)	48
Gl-Rheb degR1	CTCRATCTCSAGGATGRCTC	I (outer)	45
Gl-Rheb degR2	GATGRCTCKTGTGAAGATGTC	I (inner)	48
Gl-Rheb 3′R F1	CATCTACGACAAGATTCTCGAC	3′ (outer)	53
Gl-Rheb 3′R F2	GCAAAGTCACAGTTCCTGTAG	3′ (inner)	53
Gl-Rheb 5′R R1	ACCTGCCGTGTCCACCAGCTC	5′ (outer)	60
Gl-Rheb 5′R R2	GATCATAGCTGTCCACAAAC	5′ (inner)	60

E, primer used for expression analysis by reverse transcriptase-polymerase chain reaction (RT-PCR) or quantitative RT-PCR (qRT-PCR); I, primer used for initial amplification by RT-PCR; 3′, primer used for 3′ RACE PCR; 5′, primer used for 5′ RACE PCR; Inner or outer identifies primers used in nested PCR and their relative topology; mTOR, metazoan target of rapamycin.

Island Biological Laboratory (Towle and Smith, 2006). RNA isolation and cDNA synthesis were the same as described for *G. lateralis* above. The sequence for each open reading frame (ORF) was verified by RT-PCR using cDNA prepared as described below.

All initial cloning reactions for the above genes were PCR amplified using GoTaq Green master mix (Promega, Madison, WI, USA). After denaturing the cDNA at 96°C for 3 min, 35 cycles of PCR were completed with the following programme: 96°C for 30 s, the lowest annealing temperature of a primer pair (see Table 1) for 30 s, and 72°C for 30 s to 1 min. Final extension was for 7 min at 72°C. Amplified products, verified as single bands by 1% agarose gel electrophoresis, were purified using the GeneJet PCR Cloning kit (Fermentas, Glen Burnie, MD, USA), ligated into the pJET1.2 vector using the CloneJet PCR Cloning kit (Fermentas) and, after insert verification by PCR with vector primers, sequenced using a T7 primer (Davis Sequencing, Davis, CA, USA).

To acquire the 5′ and 3′ sequences for *Gl-Rheb*, the FirstChoice RLM-RACE kit (Applied Biosystems, Austin, TX, USA) was used according to the manufacturer's instructions. RACE conditions were as follows: 0.4 µl of RACE template cDNA was used in each reaction, with 8 pmol of each gene specific (Table 1) and kit primer, and other components identical to the initial PCR reactions (see above). After denaturation at 94°C for 3 min, 35 cycles of 94°C for 30 s, the lowest annealing temperature of a primer pair (Table 1) for 30 s, and 72°C for 30 s to 1 min, were completed. Final extension was for 7 min at 72°C. All products were cloned and sequenced as described above. The cloned coding sequences were deposited in GenBank (see Table 2 for accession numbers).

Tissue expression using endpoint PCR

Endpoint PCR was used to qualitatively assess the tissue distribution of *Gl-Rheb* (no. HM989971), *Gl-EF2* (no. AY552550), *Cm-Rheb* (no. HM989970), *Cm-EF2* (no. GU808334), *Ha-Rheb* (no. HM989972) and *Ha-EF2* (no. FJ790217) transcripts. For *G. lateralis*, endpoint PCR used the same samples used previously to analyze *Gl-Mstn* and *Gl-EF2* tissue expression in Covi et al. (Covi et al., 2008). For *C. maenas*, RNA was isolated from various tissues as described (Covi et al., 2010). Tissues were harvested from one intermolt adult male, except for Y-organ, eyestalk ganglia and thoracic ganglia, which were pooled from three intermolt males. For *H. americanus*, the analysis used the same samples from an intermolt female adult lobster from a previous study (MacLea et al., 2010). Reactions contained 1 µl of template cDNA and 5 pmol each of the appropriate expression primers (Table 1) in GoTaq Green master mix (Promega). After denaturation at 94°C for 3 min, 28–35 cycles of 94°C for 30 s, the lowest annealing temperature of a primer pair (Table 1) for 30 s, and 72°C for 30 s, were completed. Final extension was for 7 min at 72°C. *Ha-Rheb* used 29 and 35 cycles, *Ha-EF2* and *Cm-EF2* used 28 cycles, *Cm-Rheb* used 29 cycles, *Gl-EF2* used 30 cycles and *Gl-Rheb* used 35 cycles. After PCR was terminated, products were separated on a 1% agarose gel containing TAE (40 mmol l^{-1} Tris acetate and 2 mmol l^{-1} EDTA, pH 8.5). The gels were stained with ethidium bromide and visualized with an ultraviolet (UV) light source. All PCR products were sequence verified.

Quantification of Rheb, mTOR, s6k and Akt expression in skeletal muscles

Samples and methods for RNA isolation and cDNA synthesis were the same as described in Covi et al. (Covi et al., 2010). A LightCycler 480 thermal cycler (Roche Applied Science, Indianapolis, IN, USA) was used to quantify the levels of *Gl-Rheb* (HM989971), *Gl-mTOR* (HM989973), *Gl-Akt* (HM989974) and *Gl-s6k* (HM989975) mRNAs in claw closer and thoracic (weighted and unweighted) muscles. Reactions consisted of 1 µl of first-strand cDNA or standard, 5 µl of 2× SYBR Green I Master mix (Roche Applied Science), 5 pmol each of forward and reverse primers (Table 1) and 3 µl of nuclease-free water. PCR conditions were as follows: an initial denaturation at 95°C for 5 min, followed by 45 cycles of denaturation at 95°C for 10 s, annealing at 62°C for 20 s and extensions at 72°C for 20 s, followed by melting curve analysis of the PCR product. Transcript concentrations were determined by use of the LightCycler 480 software (Roche Applied Science, version 1.5) using a series of double-stranded DNA (dsDNA) gene standards produced by serial dilutions of PCR product for each gene (10 ag µl^{-1} to 10 ng µl^{-1}). The absolute amounts of transcript in copy numbers per µg of total RNA in the cDNA synthesis reaction were calculated based on the standard curve and the calculated molecular weight of dsDNA products. All fold changes in expression indicated in the text refer to changes in the raw expression levels of the genes.

Statistical analyses and software

Statistical analysis was performed using JMP 5.1.2, 6.0.0 or 8.0.2 (SAS Institute, Cary, NC, USA). Group variances were analyzed using a Brown–Forsythe test and found to be equal (P<0.05). Means for different developmental stages were compared using analysis of variance (ANOVA). All data not plotted as individual points are represented as means ± 1 s.e.m. and the level of significance was set at α=0.05. Paired t-tests were used for comparisons of the weighted and unweighted thoracic muscle mean comparisons, with the same α-level for significance. Spearman's rank correlation analysis and linear regression analysis of log-transformed data were performed using Excel 2007 (Microsoft Corporation, Redmond, WA, USA) and JMP (SAS Institute). The slopes of each regression line were compared with y=0 by ANOVA and P-values are reported in the relevant figures and text, along with the Spearman correlation values (ρ) and their corresponding P-values. Multiple sequence alignments were produced with ClustalX version 2.0.12 (Thompson et al., 1997) using deduced amino acid sequences. Grapher 8.2.460 (Golden Software, Golden, CO, USA), Excel and Illustrator 10

Table 2. cDNAs encoding crustacean mTOR signaling components

cDNA	Accession number	Source	Completeness	Size (bp)	Protein domain(s)	Identity/similarity to human
Gl-Rheb	HM989971	RT-PCR	Complete, except partial 3′UTR	969	Complete ORF	64% (83%)
Cm-Rheb	HM989970	EST	Complete	1543	Complete ORF	66% (81%)
Ha-Rheb	HM989972	EST	Complete	1577	Complete ORF	64% (82%)
Gl-Akt	HM989974	RT-PCR	Partial	1461	Kinase/pleckstrin domains	60% (77%)
Gl-mTOR	HM989973	RT-PCR	Partial	1050	Kinase domain	69% (80%)
Gl-s6k	HM989975	RT-PCR	Partial	1068	N-terminal kinase domain	74% (84%)

Cm, *Carcinus maenas*; Gl, *Gecarcinus lateralis*; Ha, *Homarus americanus*; EST, expressed sequence tag; RT-PCR, reverse transcriptase-polymerase chain reaction; ORF, open reading frame; UTR, untranslated region; mTOR, metazoan target of rapamycin.

```
cgcggatccgaacactgcgtttgctggctttgatgaagagagtgacgccatcaccgccacc  61
 aaaacaaacccacacctccacctgtgtttccgggcacctcaggcgcacccaggggcccca 121
 ggtgtgttgcgagctactcttatggaccactgagcatctctccacgcagccatgcctccc 181
                                                    M  P  P
 aagacgagaaaagtggccgttatgggctacagaagcgtggggaagtcatctctatgcatt 241
  K  T  R  K  V  A  V  M  G  Y  R  S  V  G  K  S  S  L  C  I
 cagtttgttgatggccagtttgtggacagctatgatcccaccattgaaaacaccttcaca 301
  Q  F  V  D  G  Q  F  V  D  S  Y  D  P  T  I  E  N  T  F  T
 aaaaaactcaaggtgcgagggcaggaatatggcctggagctggtggacacggcaggtcag 361
  K  K  L  K  V  R  G  Q  E  Y  G  L  E  L  V  D  T  A  G  Q
 gatgagtatagcatcttcccagcccaatactccatgaacatccacggctatgtcctggtc 421
  D  E  Y  S  I  F  P  A  Q  Y  S  M  N  I  H  G  Y  V  L  V
 tactccatcacctcggaaaagtccttcgaggtagcccaggtcatctatgacaagattctc 481
  Y  S  I  T  S  E  K  S  F  E  V  A  Q  V  I  Y  D  K  I  L
 gacgtgatgggcaaagtcacagttcctgtggtgttggtgggcaacaagaatgacttgcac 541
  D  V  M  G  K  V  T  V  P  V  V  L  V  G  N  K  N  D  L  H
 ctggagcgtgtggtgagcaccgaccagggcgccgcgtggcagacaactggaaggctgtg 601
  L  E  R  V  V  S  T  D  Q  G  R  R  V  A  D  N  W  K  A  V
 tttcttgagacaagtgccaaggagcatgaggcagtgagtgacatcttcactcgagccatc 661
  F  L  E  T  S  A  K  E  H  E  A  V  S  D  I  F  T  R  A  I
 ctggagattgagaaggctgatgggaacctgccctccggtaacggctgtagtatttcatga 721
  L  E  I  E  K  A  D  G  N  L  P  S  G  N  G  C  S  I  S  *
 agcctctgtgatatagccagaacctttattgccaccacctctctgacaaccgatttggat 781
 cttgaaaacaagactttgtacatggcttattctcttcacgggcaacaggatccagaaatt 841
 tgtgttttcttctgttgtatcagttctttatggccttgcctgttgtgagtatgagccagc 901
 ccactggacccatgcagtaccctcctagtctgttgtgggataatggtcagtactgttggc 961
 agtgggtg                                                     969
```

Fig. 1. Nucleotide and deduced amino acid sequences of the *Gecarcinus lateralis* Rheb (*Gl-Rheb*; GenBank accession HM989971) cDNA, including a complete 5′ untranslated region (UTR) and an incomplete 3′ UTR. The five G boxes involved in GTP binding are indicated in bold, and the lipid modification site is shown in italics. The stop codon is indicated with an asterisk.

(Adobe Systems, San Jose, CA, USA) were used for constructing/annotating graphs and figures. *In silico* analysis of predicted RNA characteristics was completed using RNAz (http://rna.tbi.univie.ac.at/RNAz) (Gruber et al., 2007), RNA analyzer (http://wb2x01.biozentrum.uni-wuerzburg.de/) (Bengert and Dandekar, 2003) and UTRscan (http://itbtools.ba.itb.cnr.it/utrscan) (Mignone et al., 2005). Estimated protein molecular weights were calculated using the Compute pI/MW tool (http://expasy.ch/tools/pi_tool.html).

RESULTS

Cloning and characterization of crustacean *Rheb* cDNAs

BLAST searches identified clones of the *Rheb* gene among EST libraries for *C. maenas* (*Cm-Rheb*) and *H. americanus* (*Ha-Rheb*) (Table 2). A BLAST search also identified a *Rheb* ortholog from a suppression subtractive hybridization cDNA library of the green mud crab, *Scylla paramamosain* (*Sp-Rheb*, ACY66406; incorrectly annotated as Ras). The *Gl-Rheb* cDNA (969 bp) contained the 5′ untranslated region (UTR), complete ORF and an incomplete 3′ UTR, when compared with the 3′ UTRs in the *Ha-Rheb* and *Cm-Rheb* cDNA sequences (Fig. 1, Fig. 4, Table 2). All four decapod *Rheb* cDNAs encoded 182-amino acid proteins with estimated masses of 20.2 kDa for *Gl-Rheb* and 20.4 kDa for *Cm-Rheb*, *Sp-Rheb* and *Ha-Rheb*.

The deduced amino acid sequences of the four crustacean Rheb proteins were highly conserved, showing high identity and similarity to each other and to Rheb protein sequences in insects and human (Fig. 2). The decapod Rheb sequences were aligned with other arthropod sequences (human body louse and red flour beetle), as well as the human Rheb amino acid sequence. A different paralog

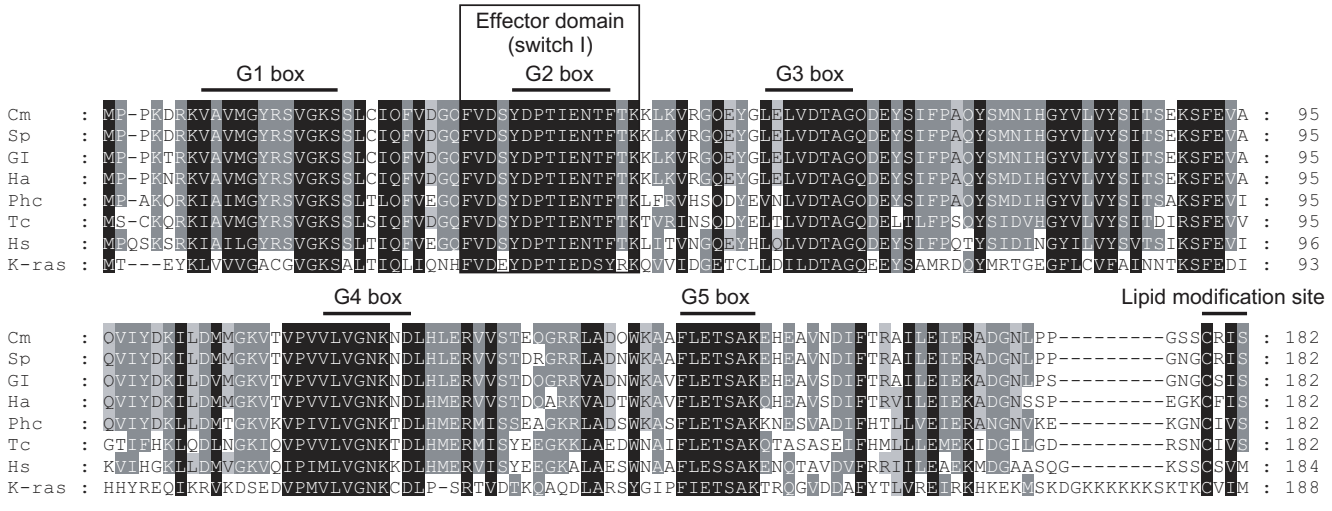

Fig. 2. Multiple alignment of deduced amino acid sequences for Rheb proteins in four crustacean species, two insect species and human, compared with the human paralog K-ras. Abbreviations: green crab, *Carcinus maenas* (Cm; GenBank HM989970); green mud crab, *Scylla paramamosain* (Sp, ACY66406); blackback land crab, *Gecarcinus lateralis* (Gl; HM989971); American lobster, *Homarus americanus* (Ha; HM989972); human body louse, *Pediculus humanis corporis* (Phc, XP_002422596); red flour beetle, *Tribolium castaneum* (Tc; XP_970662); human Rheb, *Homo sapiens* (Hs, NP_005605); and human K-ras (K-ras, AAB41942). *Gl-Rheb* is identical/similar to the other sequences at these levels: Cm (93%/96%), Sp (95%/97%), Ha (91%/93%), Hs (64%/83%) and K-ras (41%/60%). Dashes indicate gaps introduced to optimize the alignment. G boxes and lipid modification site are indicated. The effector domain (switch I region), responsible for interactions with the metazoan target of rapamycin (mTOR), FKBP38 and other proteins (Aspuria and Tamanoi, 2004; Ma et al., 2008), is indicated.

within the Ras gene family (human K-ras) was included as an 'outgroup' for comparison purposes. Sequence identity was particularly high within the 'G box' motifs (G1–G5) in all the Rheb proteins. The C-terminal lipid modification site was also conserved in the arthropod Rhebs. There was less identity/similarity between the Rheb and K-ras sequences, particularly in the G1 and G2 motifs (Fig. 2). The segregation of Rheb and Ras into two distinct gene families was confirmed by phylogenetic analysis (Fig. 3). Bootstrapping values indicated a high degree of relatedness among the four decapod Rheb sequences and among the Ras-like sequences from human and insects. Bootstrapping values were lower between the crustacean and insect Rheb sequences. The multiple sequence alignment between translated crustacean, insect and human Rheb protein sequences (Fig. 2) showed significant sequence divergence outside of the G box motifs, in particular the regions between the G2 and G3 boxes and the regions flanking the G5 box.

Multiple alignment of the nucleotide sequences identified highly conserved regions in the 3′ UTRs of the four decapod *Rheb* cDNAs (Fig. 4). Putative functional elements in the 3′ UTR were identified using RNA analysis software (see Materials and methods). A poly A signal sequence (AATAAA) was identified in *Cm-Rheb* and *Ha-Rheb*, indicating that these cDNAs contained a complete 3′ UTR. The nucleotide sequences of the *Cm-Rheb* and *Ha-Rheb* were 47% identical, with the greatest amount of identity in the first ~275 nucleotides of the 3′ UTR. A K-box sequence (TGTGAT) (Lai et al., 1998) was located six nucleotides after the stop codon in all four decapod *Rheb* cDNAs (Fig. 4). Among the other arthropod species for which complete Rheb sequences are available (e.g. copepod, sand fly, silkworm and mosquito), however, no K-box sequence was found in the 3′ UTR. Among the mammalian sequences in GenBank, the K-box is generally absent. Only human (NM005614) and cattle (NM001031764) Rheb sequences contain a K-box, which overlaps with the stop codon. A ~100-nucleotide region (nucleotides #161 to #264 in the *Cm-Rheb* 3′ UTR) was predicted to form a stem-looped secondary structure consistent with mRNAs (see Materials and methods).

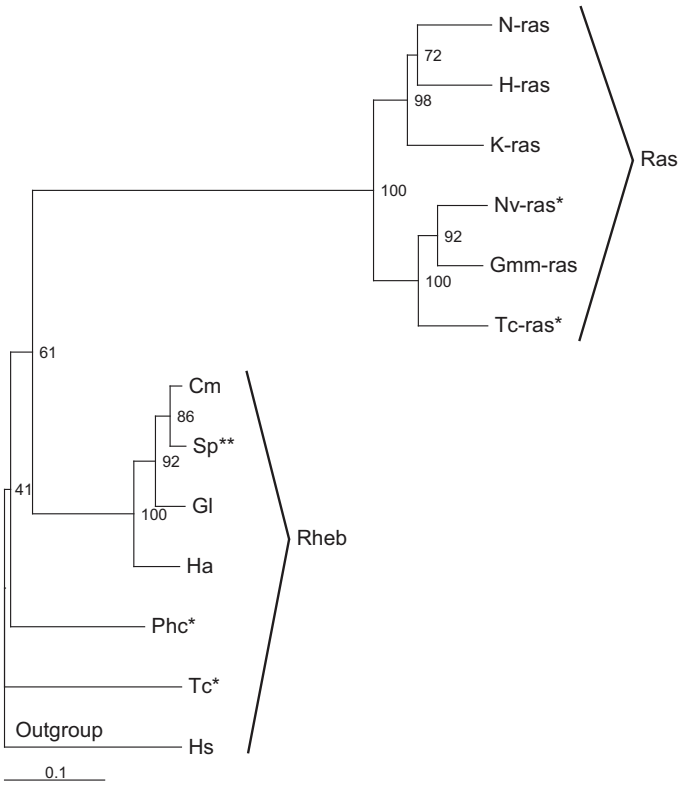

Fig. 3. Phylogenetic analysis of vertebrate and invertebrate Rheb-like proteins compared with other Ras family members. The deduced protein sequences were used to construct the tree and bootstrap values are indicated at each node; human Rheb (Hs) served as the outgroup. Rheb-like proteins of the Ras superfamily showed greater similarity to each other than to sequences from human Ras genes (H-ras, K-ras and N-ras) or Ras-like sequences in other species. Abbreviations: for Rheb-like protein sequences and human K-ras, see Fig. 2 legend. For other Ras-like sequences: *Homo sapiens* (N-ras, NP_002515; H-ras, NP_001123914; K-ras, AAB41942), jewel wasp, *Nasonia vitripennis* (Nv-ras; XP_001606521), tsetse fly, *Glossina morsitans morsitans* (Gmm-ras; ADD19793) and red flour beetle, *Tribolium castaneum* (Tc-ras; XP_974600). Asterisk (*) indicates sequences predicted from genomic data; all other sequences originate from cDNA. Double asterisk (**) indicates sequences derived from previously uncharacterized expressed sequence tags (ESTs). The scale bar represents the proportion of amino acid differences between sequences based on nucleotide substitutions per site.

Endpoint RT-PCR showed that Rheb and EF2 were ubiquitously expressed (Fig. 5). *Cm-Rheb* and *Cm-EF2* transcripts were present in skeletal muscle, gill, hindgut, hepatopancreas, heart, midgut, testis, thoracic ganglion and Y-organ (Fig. 5A). *Gl-Rheb* and *Gl-EF2* transcripts were present in skeletal muscle, hindgut, heart, eyestalk ganglion, thoracic ganglion and Y-organ (Fig. 5B). *Ha-Rheb* and *Ha-EF2* were present in antennal gland, skeletal muscle, hindgut, hepatopancreas, heart, midgut, ovary and thoracic ganglion (Fig. 5C).

Cloning of cDNAs encoding *Gl-mTOR*, *Gl-Akt* and *Gl-s6k*

cDNAs encoding additional components of the mTOR signaling pathway were cloned from *G. lateralis* tissues using RT-PCR. Partial sequences for *Gl-Akt*, *Gl-mTOR* and *Gl-s6k* were obtained (Table 2). The deduced sequences shared high degrees of identity and similarity to the human ortholog of each cDNA at the protein level (60–74% identity/77–84% similarity; Table 2), with even higher identity and similarity to orthologs in insects (data not shown). The *Gl-mTOR* partial cDNA encoded the kinase domain, which is located near the 3′ end of the ORF in the human mTOR (reviewed by Abraham and Wiederrecht, 1996). *Gl-Akt* encoded the kinase and pleckstrin domains, and *Gl-s6k* encoded both kinase domains and the substrate-binding region (Table 2).

Effects of ESA on the expression of mTOR signaling components in claw and weighted thoracic muscles

qPCR was used to analyze levels of land crab mTOR signaling components in claw and thoracic muscles as animals progressed through the molt cycle. The same cDNA samples from Covi et al. (Covi et al., 2010) were used in the analysis. 'Weighted' thoracic muscle served as an internal control, as this muscle does not atrophy during premolt. The data were graphed as a function of three variables: time, R-index and molt stage. Events post-ESA or post-ecdysis were measured in time after the treatment or event. The R-index was used to compare the two methods (ESA and MLA) of molt induction. Finally, a molt stage classification, as applied to *G. lateralis* by Skinner (Skinner, 1962), was used to integrate the data from time and R-index. Molt induction increased hemolymph ecdysteroid titers; the data from Covi et al. (Covi et al., 2010) are reproduced in Fig. 6E and Fig. 7E to compare gene expression with hemolymph ecdysteroid titer.

The expression of *Gl-Akt*, *Gl-Rheb*, *Gl-mTOR* and *Gl-s6k* each responded differently to molt induction by ESA (Fig. 6A–D). The expression of a 'housekeeping' gene, *Gl-EF2*, is for the most part expressed at constant levels, except at 20 days post-ESA, when levels

Fig. 4. Nucleotide alignment of 3′ untranslated region (UTR) for four crustacean Rheb genes. Abbreviations: green crab, *Carcinus maenas* [Cm, complete, 872 nucleotides (nt)]; green mud crab, *S. paramamosain* (Sp, partial 3′ UTR, 81 nt); blackback land crab, *Gecarcinus lateralis* (Gl, partial 3′ UTR, 248 nt); and American lobster, *Homarus americanus* (Ha, complete, 883 nt). Identities among at least two sequences are indicated with black shading. Dashes indicate gaps introduced to optimize the alignment, but gaps at the ends of sequences were removed for clarity. All sequences begin immediately 3′ of the stop codon. Conserved K-box (minimal consensus TGTGAT) and poly A signal (AATAAA) sequences are labeled. The portion of the alignment between the @ symbols indicates the portion of the RNA (160–280 of *Cm-Rheb*) predicted by RNAz (Gruber et al., 2007) to form secondary structure consistent with coding mRNA. ORF, open reading frame.

increase 2.1-fold in claw muscle but not in thoracic muscle (Covi et al., 2010). *Gl-Akt* showed a similar pattern of expression in both muscle types (Fig. 6A). *Gl-Akt* mRNA level increased 1.8-fold in claw muscle and 3.5-fold in thoracic muscle by 7 days post-ESA (R=10.0). From these peak levels, *Gl-Akt* decreased 2.6-fold in claw muscle and 2.4-fold in thoracic muscle by 20 days post-ESA (R=19.9).

ESA had a differential effect on the expression of *Gl-Rheb* in claw and thoracic muscles (Fig. 6B). A lower level of *Gl-Rheb* in thoracic muscle from intact animals contributed to an immediate 3.4-fold increase 1 day post-ESA (R=6.6). However, *Gl-Rheb* expression in thoracic muscle was relatively constant during premolt. By contrast, *Gl-Rheb* mRNA in claw muscle increased 3.9-fold over the level in intact animals at 7 days post-ESA (R=10.0) and remained elevated at 14 days (R=15.5) and 20 days (R=19.9) post-ESA. *Gl-Rheb* transcript levels in claw muscle were significantly higher than those in thoracic muscle at every molt stage, except 1 and 3 days post-ESA (Fig. 6B, asterisks).

ESA increased *Gl-mTOR* mRNA levels but the timing of the peaks differed between the two muscle types (Fig. 6C). In claw muscle, a maximum level occurred at 7 days (R=10.0) post-ESA, which was 2.8-fold higher than the level in intact animals; mRNA levels remained elevated at 14 days and 20 days post-ESA (R=15.5 and 19.9, respectively). In thoracic muscle, a maximum occurred at 14 days post-ESA, which was 2.4-fold higher than intact animals. However, unlike claw muscle, thoracic muscle *Gl-mTOR* mRNA levels decreased 2.5-fold after the 14 days post-ESA peak, returning to a level comparable to that from the intact animals. At two points in the molt cycle (R=10.0 and 19.9), *Gl-mTOR* mRNA levels were

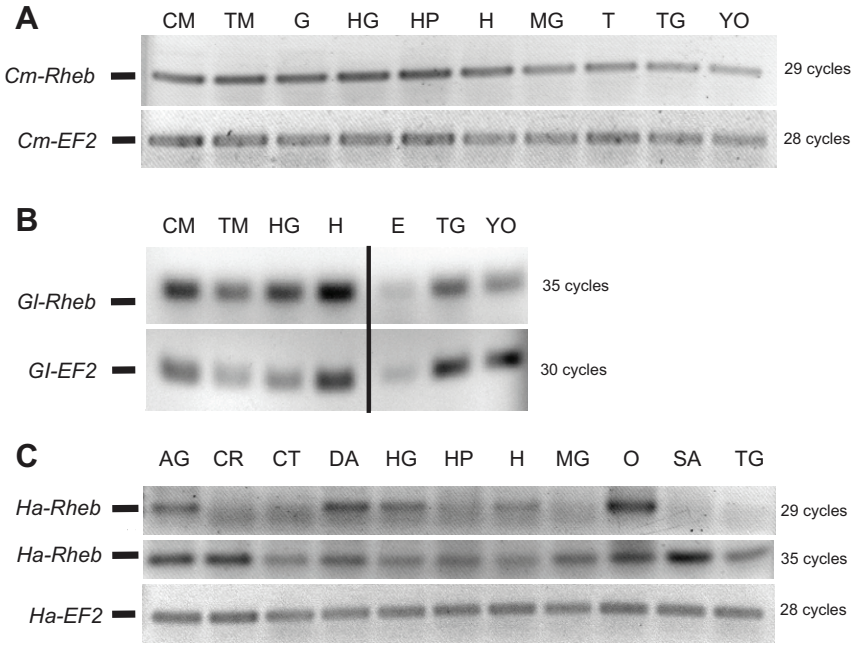

Fig. 5. Qualitative expression of three Rheb orthologs in crustacean tissues using endpoint reverse transcriptase-polymerase chain reaction (RT-PCR) resolved by agarose gel electrophoresis. Representative inverse images of ethidium bromide-stained gels are shown. (A) *Cm-Rheb* (281 bp product) and *Cm-EF2* (278 bp) expression in various tissues. (B) *Gl-Rheb* (119 bp product) and *Gl-EF2* (229 bp) expression. (C) *Ha-Rheb* (119 bp product—after either 29 or 35 cycles of PCR) and *Ha-EF2* (229 bp) expression. Elongation factor 2 (EF2) served as a constitutively expressed control in each crustacean species and was expressed at similar levels in all tissues. In B, a vertical line indicates different portions of the same gel that were placed next to each other for visual comparison with A and C. Abbreviations: AG, antennal gland (lobster); CM, claw muscle (crabs); CR, crusher claw closer muscle (lobster); CT, cutter claw closer muscle (lobster); DA, deep abdominal muscle (lobster); E, eyestalk ganglia (all); G, gill (all); H, heart (all); HG, hindgut (all); HP, hepatopancreas (all); MG, midgut (all); O, ovary (all except Cm); SA, superficial abdominal muscle (lobster); T, testis (all except lobster); TG, thoracic ganglion (all); TM, thoracic muscle (crabs); and YO, Y organ (molting gland, all).

significantly lower in thoracic muscle than in claw muscle (Fig. 6C, asterisks).

ESA had small effects on the expression of *Gl-s6k* in both muscle types (Fig. 6D). In claw muscle, there were no changes in *Gl-s6k* transcript levels, except for a 1.9-fold increase over intact levels at 7 days post-ESA. In thoracic muscle, *Gl-s6k* expression in intact animals was lower than that in claw muscle but was expressed at similar levels to claw muscle in premolt animals, except at 7 days post-ESA. Thoracic muscle *Gl-s6k* expression was significantly higher in ESA animals than in intact animals. There was little change in the expression of *Gl-s6k* in thoracic muscle during premolt, except for a small increase and subsequent decrease 10–20 days post-ESA.

Effects of MLA on the expression of mTOR signaling components in claw and weighted thoracic muscles

The expression of *Gl-Akt*, *Gl-Rheb*, *Gl-mTOR* and *Gl-s6k* each responded differently to molt induction by MLA (Fig. 7A–D). Animals entered premolt, as measured by the R-index, and successfully molted. Thus, we were able to compare gene expression in muscles from premolt and post-molt animals. *Gl-EF2* mRNA levels showed no significant changes in the same samples (Covi et al., 2010). *Gl-Akt* was expressed at constant levels in thoracic muscle, except at mid-premolt (R=15.0), where a significant 1.9-fold increase over intact animals was observed (Fig. 7A). By contrast, *Gl-Akt* was expressed in claw muscle at the same levels in intact (intermolt), early premolt (R=10.0) and mid-premolt (R=15.0) stages and then decreased 2.8-fold by 10 days post-molt (Fig. 7A). *Gl-Akt* mRNA levels in thoracic muscle were significantly lower than those in claw muscle from intact and premolt animals (Fig. 7A, asterisks); the means were not significantly different at 2 days and 10 days post-molt.

MLA had differential effects on *Gl-Rheb* expression in claw and thoracic muscles. In claw muscle, *Gl-Rheb* mRNA levels increased during premolt, reaching a level 3.4-fold higher in late premolt animals (R=23.5) than that in intermolt (intact) animals (Fig. 7B). Following ecdysis, *Gl-Rheb* mRNA levels decreased and returned to intermolt levels by 10 days post-molt. By contrast, thoracic muscle showed a small increase in *Gl-Rheb* expression during premolt; *Gl-Rheb* mRNA levels in late premolt animals (R=23.5) were 1.7-fold higher than the level in intact animals (Fig. 7B). *Gl-Rheb* mRNA levels in thoracic muscles from post-molt animals were ~2-fold higher than intact animals. *Gl-Rheb* expression in thoracic muscle was significantly lower than claw muscle at all molt stages (Fig. 7B, asterisks).

MLA had transient effects on the expression of *Gl-mTOR* in both muscle types. In claw muscle, *Gl-mTOR* mRNA levels were constant during premolt and then decreased 3.1-fold from intact levels by 10 days post-molt (Fig. 7C). In thoracic muscle, expression of *Gl-mTOR* decreased 2-fold in mid-premolt animals compared with intact animals (Fig. 7C; R=15.0). However, thoracic muscle levels returned to the initial level by late premolt (R=23.5) and decreased 1.7-fold in post-molt animals. There was no significant difference in the *Gl-mTOR* mRNA levels between claw and thoracic muscles at each molt stage, except at 10 days post-molt, in which the level in the claw was significantly lower than that in the thoracic muscle (Fig. 7C, asterisk).

The general pattern of *Gl-s6k* expression was similar between claw and thoracic muscles over the molt cycle. MLA had little effect on *Gl-s6k* expression in both muscle types, although there were significant decreases of 1.7-fold and 1.6-fold in *Gl-s6k* mRNA levels in claw and thoracic muscles, respectively, between 2 and 10 days post-molt (Fig. 7D). In thoracic muscle, a transient 1.4-fold decrease in *Gl-s6k* expression in early premolt (R=10.0) animals was reversed at later premolt stages (Fig. 7D). *Gl-s6k* mRNA levels in thoracic muscle were significantly lower than those in claw muscle at all premolt and post-molt stages (Fig. 7D, asterisks).

Relationship between *Gl-Rheb* mRNA and hemolymph ecdysteroid levels

The levels of *Gl-Akt*, *Gl-mTOR* and *Gl-s6k* mRNAs in both muscle types were not correlated with hemolymph ecdysteroid titers in animals induced to molt by either ESA or MLA (data not shown). *Gl-Rheb* mRNA level in claw muscle was correlated significantly with hemolymph ecdysteroids in both MLA and ESA animals (Fig. 8A,B, solid lines). There was no significant correlation between *Gl-Rheb* mRNA and ecdysteroid levels in the corresponding weighted thoracic muscles (Fig. 8A,B, dashed lines).

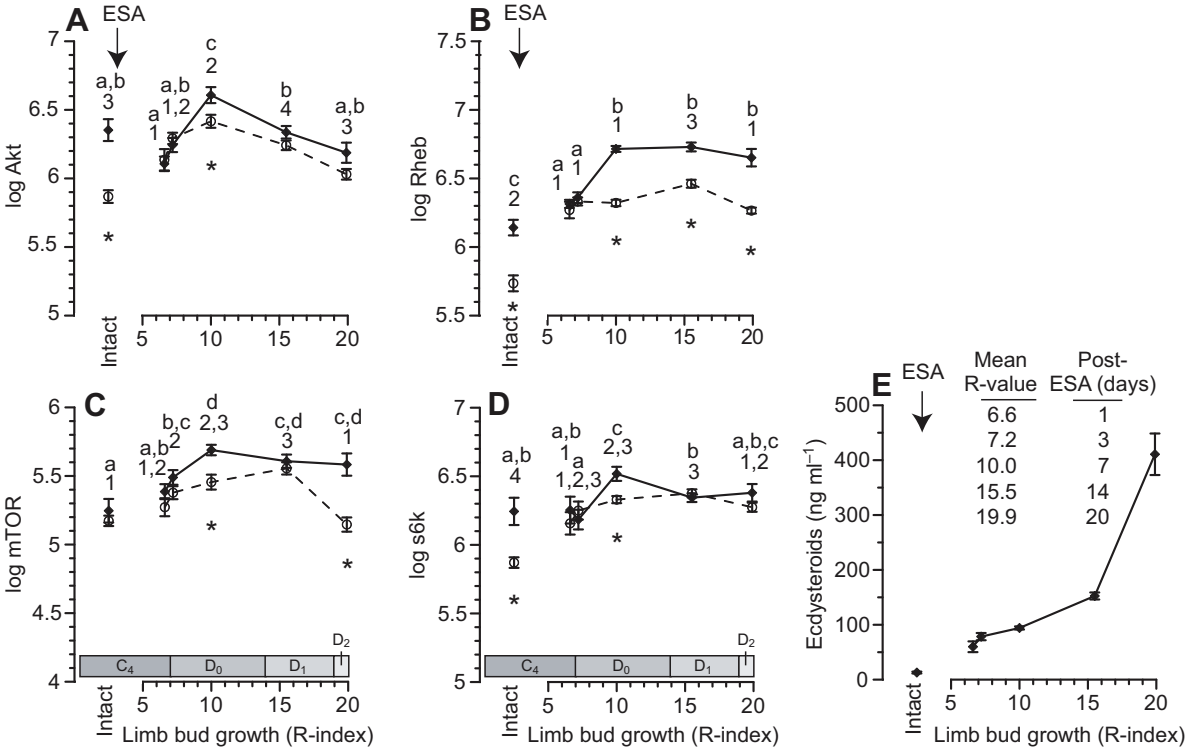

Fig. 6. Effects of eyestalk ablation (ESA) on the metazoan target of rapamycin (mTOR) pathway gene expression in claw and weighted thoracic muscles and hemolymph ecdysteroid levels. Abundance of mRNA transcripts (copies μg^{-1} total RNA), quantified by quantitative reverse transcriptase-polymerase chain reaction (qRT-PCR), is plotted as a function of R-index for *Gl-Akt* (A), *Gl-Rheb* (B), *Gl-mTOR* (C) and *Gl-s6k* (D). Intermolt animals are plotted as separate data points to the left of the R-index scale (intact). There are no post-molt data, as ESA animals do not survive molt. Thoracic muscle: open circles and a dashed line. Claw muscle: closed diamonds and a solid line. Standard error measurements for R-index means are not displayed but are ≤0.3. Shared letters indicate no significant difference for multiple comparisons among claw muscle data. Shared numbers indicate no significant difference for multiple comparisons among thoracic muscle data. Asterisks indicate a significant difference between claw and thoracic muscle means at the same molt stage. Scales for ordinates are identical but ranges are shifted to accommodate varied levels of expression of different genes. Corresponding molt stages are given above the abscissa in C and D. (E) Hemolymph ecdysteroid titers data are from Fig. 3A in Covi et al. (Covi et al., 2010). Data are expressed as a function of R-index; inset in E delineates the relationship between R-index and time following ESA. All data are presented as means ± s.e.m. (*N*=11–12.)

Relationship between *Gl-Rheb* mRNA and *Gl-Mstn* mRNA levels

Gl-Rheb transcript level was quantified using the same cDNA samples as those used for quantifying the *Gl-Mstn* transcript (Covi et al., 2010). Given the negative correlation of *Gl-Mstn* expression with ecdysteroids reported in Covi et al. (Covi et al., 2010) and the positive correlation of *Gl-Rheb* expression with ecdysteroid levels in this study (see above), we expected a negative correlation between *Gl-Rheb* and *Gl-Mstn* mRNA levels, indicating a linkage between *Gl-Mstn* and *Gl-Rheb* expression. However, a negative correlation was not consistently observed (Fig. 9). In MLA animals, the *Gl-Mstn* and *Gl-Rheb* transcript copy numbers in claw muscle were not significantly correlated (Fig. 9A). In ESA animals, however, there was a weak negative correlation between *Gl-Mstn* and *Gl-Rheb* mRNA levels that was statistically significant (Fig. 9B). By contrast, *Gl-Rheb* mRNA level was positively correlated with *Gl-Mstn* mRNA level in thoracic muscle from ESA and MLA animals (Fig. 9A,B). Both positive correlations in thoracic muscle were statistically significant.

Effects of unweighting on gene expression in thoracic muscle

The expression of mTOR components was quantified in the same cDNA samples from Covi et al. (Covi et al., 2010). In intact (intermolt) animals, unweighting increased *Gl-Rheb* mRNA level 2.2-fold and *Gl-s6k* mRNA level 1.3-fold; there was no effect of unweighting on the expression of *Gl-Akt* and *Gl-mTOR* (Fig. 10A). *Gl-Rheb* was expressed at significantly higher levels in unweighted thoracic muscle than weighted thoracic muscle expression over the molt cycle (Fig. 10B, asterisks). *Gl-Rheb* expression in unweighted thoracic muscle remained elevated during premolt (Fig. 10B). There were small increases of 1.3-fold and 1.4-fold over intermolt levels at 2 and 10 days post-molt, respectively. The expression of *Gl-Akt*, *Gl-mTOR* and *Gl-s6k* in unweighted thoracic muscle during the premolt and post-molt periods paralleled expression in weighted thoracic muscle (data not shown).

DISCUSSION

The insulin/mTOR signaling pathway is highly conserved in metazoans and functions as a nutrient sensor that is crucial for growth and development in insects and other invertebrates (reviewed by Hietakangas and Cohen, 2009; Soulard et al., 2009; Teleman, 2010). In order to determine its function in crustaceans, we cloned six mTOR pathway components representing four different genes from three crustacean species (Table 2). cDNAs encoding Rheb were cloned from *G. lateralis*, *C. maenas* and *H. americanus*, and deduced amino acid sequences had high identity with orthologs in other species (Figs 2 and 3; Table 2). Rheb was expressed in all tissues examined (Fig. 5), which is consistent with its ubiquitous expression in other organisms (Aspuria and Tamanoi, 2004). Partial cDNAs encoding Akt, mTOR and s6k were cloned from *G. lateralis* and

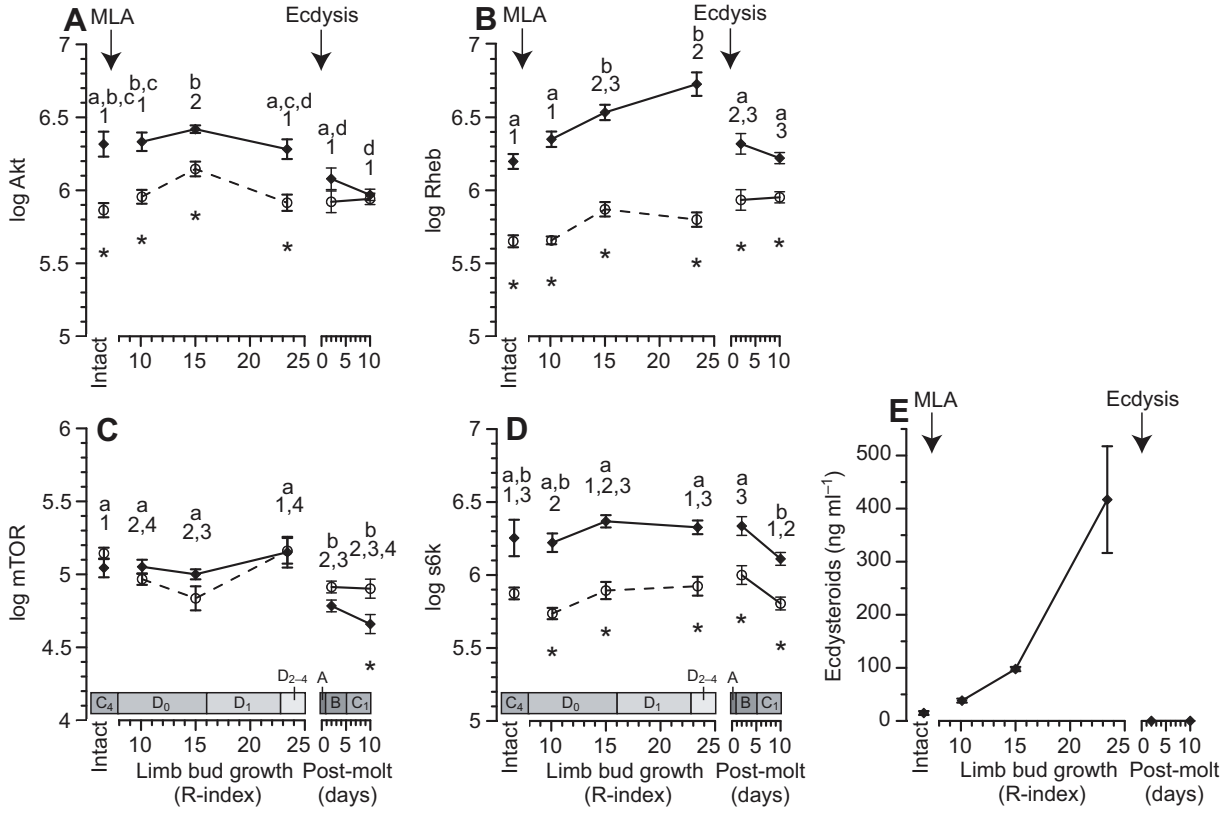

Fig. 7. Effects of multiple leg autotomy on the metazoan target of rapamycin (mTOR) pathway gene expression in claw and weighted thoracic muscles and hemolymph ecdysteroid levels. Abundance of mRNA transcripts (copies μg^{-1} total RNA), quantified by quantitative reverse transcriptase-polymerase chain reaction (qRT-PCR), is plotted as a function of R-index for premolt animals and as a function of days following ecdysis for post-molt animals for *Gl-Akt* (A), *Gl-Rheb* (B), *Gl-mTOR* (C) and *Gl-s6k* (D). Intermolt animals are plotted as separate data points to the left of the R-index scale (intact). Thoracic muscle: open circles and a dashed line. Claw muscle: closed diamonds and a solid line. Standard error measurements for R-index means are not displayed but are ≤0.5. Shared letters indicate no significant difference for multiple comparisons among claw muscle data. Shared numbers indicate no significant difference for multiple comparisons among thoracic muscle data. Asterisks indicate a significant difference between claw and thoracic muscle means at the same molt stage. Scales for ordinates are identical, but ranges are shifted to accommodate varied levels of expression of different genes. Corresponding molt stages are given above the abscissa in (C) and (D). (E) Hemolymph ecdysteroid titers data are from Fig. 4A in Covi et al. (Covi et al., 2010). Data are expressed as a function of R-index. Post-molt measurements of hemolymph ecdysteroid were <11 ng ml^{-1}; error bars are excluded for these samples because measurements were often below the detection limit for this assay of 5 ng ml^{-1}. All data are presented as means ± s.e.m. Sample sizes varied with molt stage (intact, *N*=8; R=10.1 and 15.0, *N*=12; R=23.4, *N*=9; 2 and 10 days post-molt, *N*=14).

showed high levels of sequence identity when compared with human orthologs (Table 2). This level of relatedness was even higher when compared by BLASTX against top hits among insect sequences in the database (68–81% identity and 79–89% similarity).

The decapod crustacean Rheb contained the five highly conserved 'G boxes' for GTP binding and GTPase activity and the C-terminal lipid modification site (Figs 1 and 2; CAAX, where C=Cys, A=aliphatic residue, X=any residue but usually Ala, Cys, Met, Gln or Ser) (reviewed in Aspuria and Tamanoi, 2004; Wennerberg et al., 2005), which is required for proper targeting to membranes and the downstream effects of Rheb (Castro et al., 2003). The 15-amino acid effector domain, which includes the G2 box (Fig. 2), is important for Rheb activation of mTOR (Aspuria and Tamanoi, 2004; Ma et al., 2008). The effector domain also mediates binding of Rheb to FKBP38, which is thought to inhibit mTOR activity under nutrient-poor conditions (Dunlop et al., 2009; Ma et al., 2008). However, there is contradictory evidence pertaining to the role of FKBP38 in modulating Rheb activity (Wang et al., 2008).

Sequence alignment of the 3′ UTR identified several highly conserved regions in the crustacean Rheb cDNAs (Fig. 4). Of particular interest was the potential regulation of Rheb by the K-box motif (TGTGAT). The K-box was first identified in *Drosophila melanogaster*, where it functions in Notch signaling (Lai et al., 1998). Although this motif is absent from many arthropod Rheb genes (e.g. those in copepods, sand fly, silkworm and several mosquitoes) and many mammalian Rheb genes, except human (NM_005614) and cattle (NM_001031764), the complete identity within the decapod Rhebs suggests that the K-box is an important regulatory element in this group of organisms. Other studies have shown that the K-box is regulated by microRNAs in *Drosophila* and mouse (Lai et al., 2005; Wu et al., 2008). This motif is also important for development in the silkworm (Zeng et al., 2009) and is present in the 3′ UTR of cyclin B in the Chinese mitten crab, *Eriocheir sinensis* (Fang and Qiu, 2009). Given the successful application of RNAi technology in crustaceans (reviewed in Shekhar and Lu, 2009) and the presence of the microRNA machinery in shrimp (Su et al., 2008), it is likely that post-transcriptional regulation of crustacean Rheb is mediated by microRNAs that may target the K-box motif.

Two molt induction methods were used to determine the effects of ecdysteroids on the expression of mTOR signaling components. Both methods increase hemolymph ecdysteroid titers but over

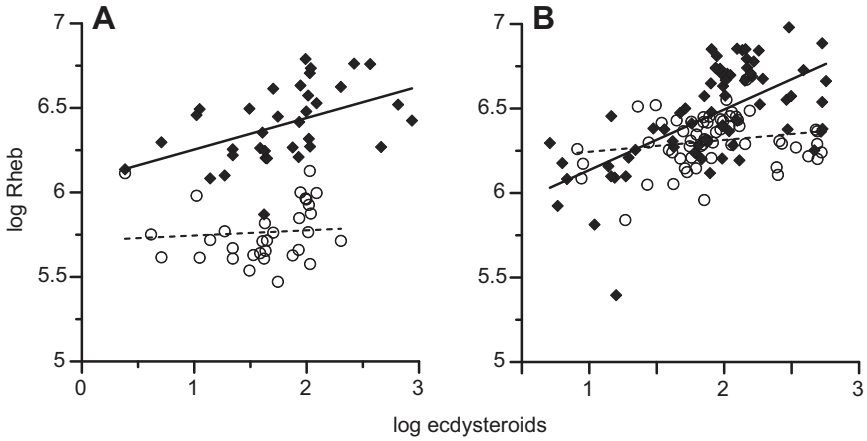

Fig. 8. Relationship between *Gl-Rheb* mRNA and hemolymph ecdysteroid levels. Regressions of *Gl-Rheb* log-transformed transcript abundance (copies μg^{-1} total RNA) *vs* ecdysteroid titer ($pg\,\mu l^{-1}$) include all the intermolt and premolt data in Fig. 6B and Fig. 7B for thoracic muscle (open circles and dashed line) and claw muscle (closed diamonds and solid line) from animals stimulated to molt by multiple leg autotomy (MLA) (A) or eyestalk ablation (ESA) (B). Spearman rank correlation coefficients (ρ), *P*-values for these correlations, coefficients of linear regression and *P*-values for ANOVA comparison to $y=0$ are: (A) claw muscle, ρ=0.5661, $P=0.0004$, $R^2=0.2191$ and $P=0.0046$; thoracic muscle, ρ=0.2630, $P=0.1458$, $R^2=0.0021$ and $P=0.6451$; and (B) claw muscle, ρ=0.6134, $P<0.0001$, $R^2=0.3771$ and $P<0.0001$; thoracic muscle, ρ=–0.0514, $P=0.6842$, $R^2=0.0382$ and $P=0.6564$.

different temporal scales (Skinner, 1985). ESA increased ecdysteroid level by 1 day post-ESA; animals entered premolt within a few days and reached late premolt (Stage D_2) 20 days post-ESA (Fig. 6E). Animals molt ~25 days post-ESA (Skinner and Graham, 1972). However, ESA animals experience a 100% mortality at ecdysis, indicating that an acute elevation of ecdysteroid does not mimic a natural molt (Covi et al., 2010; Skinner and Graham, 1972). By contrast, animals tolerate MLA well and all successfully molt (Covi et al., 2010; Skinner and Graham, 1972). Animals enter premolt several weeks after MLA, which allows time for the basal limb regenerates to differentiate (Mykles, 2001). Animals molt 3–4 weeks after entering premolt (Skinner and Graham, 1972). Thus, ESA animals reach ecdysis in about half the time as MLA animals (Skinner and Graham, 1972). In this study, hemolymph ecdysteroid levels increased more slowly in MLA animals than in ESA animals, when comparing animals at the same premolt stage. At R≈10 and ≈15, the ecdysteroid titers were higher in ESA animals than in MLA animals; by late premolt, the titers were the same (compare Fig. 6E and Fig. 7E).

The only consistent effect of molt induction on mTOR pathway components was an increase in *Gl-Rheb* expression in claw muscle. ESA increased *Gl-Rheb* mRNA level 3.9-fold, which was sustained through the premolt period (Fig. 6B). MLA increased *Gl-Rheb* mRNA level during premolt, reaching a maximum in late premolt that was 3.4-fold greater than that in intact animals (Fig. 7B). By contrast, molt induction had little or no effect on *Gl-Rheb* expression in thoracic muscle (Fig. 6B and Fig. 7B). Thoracic muscle served as an internal control, as it is exposed to the same hormonal environment but does not atrophy (Griffis et al., 2001). Qualitative and quantitative differences in the expression of ecdysteroid receptor (EcR/RXR) isoforms may contribute to the differences in response of the claw and thoracic muscles to ecdysteroids (Kim et al., 2005). Moreover, there is a significant correlation between *Gl-Rheb* mRNA level in the claw muscle and the level of ecdysteroid in the hemolymph but not in the thoracic muscle (Fig. 8). These data strongly suggest that *Gl-Rheb* expression is upregulated by ecdysteroids in claw muscle.

The preferential upregulation of *Gl-Rheb* in claw muscle during premolt indicates that Rheb plays a role in regulating protein turnover in molt-induced claw muscle atrophy. As a key regulator of mTOR, Rheb stimulates protein synthesis in mammals and invertebrates (Dunlop and Tee, 2009; McCarthy and Esser, 2010; Soulard et al., 2009; Teleman, 2010). It is likely that increased *Gl-Rheb* expression is responsible, at least in part, for the increase in global protein

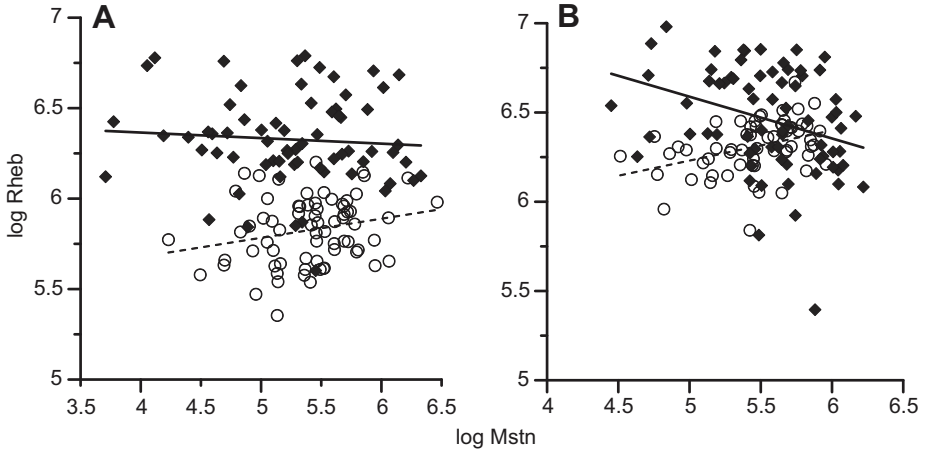

Fig. 9. Relationship between *Gl-Rheb* mRNA and *Gl-Mstn* mRNA levels. Regressions of *Gl-Rheb* transcript abundance (copies μg^{-1} total RNA) *vs* *Gl-Mstn* transcript (copies μg^{-1} total RNA) include all the intermolt and premolt data in Fig. 6B and Fig. 7B for thoracic muscle (open circles and dashed line) and claw muscle (closed diamonds and solid line) from animals stimulated to molt by multiple leg autotomy (MLA) (A) or eyestalk ablation (ESA) (B). *Gl-Mstn* data are from Covi et al. (Covi et al., 2010). Spearman rank correlation coefficients (ρ), *P*-values for these correlations, coefficients of linear regression and *P*-values for ANOVA comparison to $y=0$ are: (A) claw muscle, ρ=–0.1024, $P=0.4209$, $R^2=0.0097$ and $P=0.4394$; thoracic muscle, ρ=0.2372, $P=0.0497$, $R^2=0.0652$ and $P=0.0342$; and (B) claw muscle, ρ=–0.3442, $P=0.0033$, $R^2=0.1038$ and $P=0.0061$; thoracic muscle, ρ=0.1264, $P=0.3155$, $R^2=0.1402$ and $P=0.0029$.

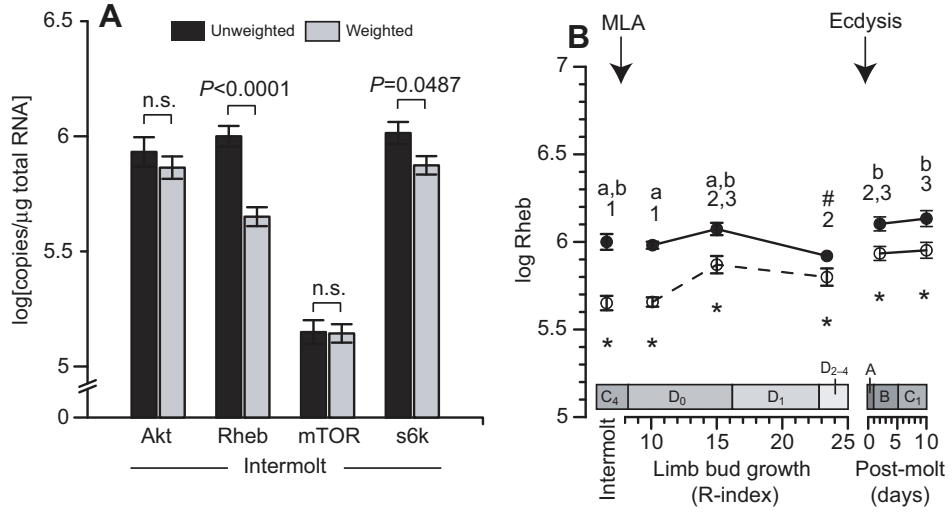

Fig. 10. Effects of unweighting on gene expression in thoracic muscle of land crabs. (A) Intermolt expression of *Gl-Akt*, *Gl-Rheb*, *Gl-mTOR* and *Gl-Akt* (copies μg^{-1} total RNA). *P*-values for significant differences are given above each pairwise comparison; n.s. indicates no significant difference at α=0.05. Data are presented as means ± s.e.m. (*N*=16–17). (B) *Gl-Rheb* expression (copies μg^{-1} total RNA) in thoracic muscles over a molt cycle induced by multiple leg autotomy (MLA). Abundance of mRNA transcripts is plotted as a function of R-index for *Gl-Rheb* as in Fig. 7. Intermolt animals are plotted as separate data points to the left of the R-index scale. Weighted thoracic muscle: open circles and a dashed line. Unweighted thoracic muscle: closed circles and a solid line. Standard error measurements for R-index means are not displayed but are ≤0.5. Shared letters indicate no significant difference for multiple comparisons among unweighted thoracic muscle data. Shared numbers indicate no significant difference for multiple comparisons among weighted thoracic muscle data. Asterisks indicate a significant difference between unweighted and weighted thoracic muscle means at the same molt stage. Corresponding molt stages are given above the abscissa. Data are presented as means ± s.e.m. Sample sizes varied with molt stage (intact, *N*=16–17; R=10.1 and 15.0, *N*=12; R=23.4, *N*=9; 2 days and 10 days post-molt, *N*=14). Only one measurement was made for the unweighted group during late premolt, and this data point in unweighted thoracic muscle is indicated by a # symbol on the graph.

synthesis in atrophic claw muscle (Covi et al., 2010). Increased *Gl-Rheb* transcription would increase the pool of Gl-Rheb protein capable of activating mTOR. This is what occurs when Rheb is overexpressed in mammalian and insect cells (Aspuria and Tamanoi, 2004; Dunlop and Tee, 2009; Hall et al., 2007; Ma et al., 2008). For example, Rheb overexpression increases translational initiation and protein synthesis in rat fibroblasts (Kubica et al., 2008). The increase in *Gl-Rheb* mRNA (Fig. 7B) parallels the increase in soluble and myofibrillar protein synthesis in animals induced to molt by MLA (Covi et al., 2010). However, the increases in *Gl-Rheb* mRNA and protein synthesis are not the same magnitudes (~4-fold *vs* 11-fold and 13-fold, respectively), indicating that mTOR-mediated protein synthesis is not regulated solely by *Gl-Rheb* transcription. Gl-Rheb is probably regulated post-transcriptionally as well. Rheb-GAP is a heterodimer of TSC1 and TSC2 subunits that inactivates Rheb by stimulating the hydrolysis of GTP to GDP. Rheb-GAP in turn is inhibited when phosphorylated by Akt (Drummond et al., 2009a; McCarthy and Esser, 2010; Teleman, 2010). Thus, activation of Akt maintains more Rheb in the activated state by inhibiting Rheb-GAP. Overexpression of a constitutively active Akt increases TSC2 phosphorylation and mTOR activity in mouse myotubes (Ohanna et al., 2005). TSC2 phosphorylation is decreased in atrophic mammalian muscle, which is consistent with the reductions in mTOR activity and protein synthesis under these conditions (Amirouche et al., 2009). Overexpression of TSC1 causes atrophy in mouse muscle by inhibiting mTOR (Wan et al., 2006). In human skeletal muscle, increased Rheb expression coincides with increased protein synthesis after resistance exercise, which is inhibited by rapamycin (Drummond et al., 2009b; Drummond et al., 2009c). Taken together, Rheb, an integral component of the mTORC1, is an important regulator of protein synthesis in mammalian and crustacean muscles. It is likely that increases in the levels of Gl-Rheb protein contribute to the large increase in global protein synthesis in premolt claw muscle (Covi et al., 2010; Skinner, 1965).

Transcription of other components of the mTOR signaling pathway in claw and thoracic muscles are not regulated strictly by ecdysteroid titer. Any changes in the mRNA levels of *Gl-Akt*, *Gl-s6k* and *Gl-mTOR* during premolt were transient (Fig. 6A,C,D and Fig. 7A,C,D), and there was no correlation of the mRNA levels with hemolymph ecdysteroid level (data not shown). It is likely that Gl-Akt, Gl-s6k and Gl-mTOR are regulated by phosphorylation. In mammals, various conditions that alter muscle mass can affect Akt, mTOR, 4E-binding protein 1 and s6k phosphorylation with little effect on total protein levels. For example, fasting or Mstn upregulation reduces phospho-Akt, phospho-TSC2, phospho-s6k and phospho-4E-binding protein 1 in mammalian muscle (Amirouche et al., 2009; Trendelenburg et al., 2009; Welle et al., 2007). Conversely, stretching and Mstn downregulation increase phospho-Akt, phospho-s6k and phospho-4E-binding protein 1 (Agata et al., 2009; Welle et al., 2009). This does not mean that molting does not influence *Gl-Akt*, *Gl-mTOR* and *Gl-s6k* expression. There were significant changes in mRNA levels as a function of molt stage and/or muscle type. However, as there were no consistent differences between claw and thoracic muscle with respect to hemolymph ecdysteroid titer, we conclude that transcriptional regulation of *Gl-Akt*, *Gl-mTOR* and *Gl-s6k* does not contribute to the increase in protein synthesis during molt-induced claw muscle atrophy.

Ecdysteroids regulate protein metabolism in the claw muscle (reviewed by Mykles, 1997; Mykles, 1999; Mykles and Skinner, 1982a). The expression of both *Gl-Rheb* and *Gl-Mstn* in claw muscle is sensitive to ecdysteroid, as indicated by the correlation between mRNA levels and hemolymph ecdysteroid titer. *Gl-Mstn* is strongly downregulated by ecdysteroid (Covi et al., 2010) whereas *Gl-Rheb*

was strongly upregulated (Fig. 8). As Mstn signaling regulates gene expression (Kollias and McDermott, 2008), ecdysteroids may increase *Gl-Rheb* expression by suppressing *Gl-Mstn* expression, resulting in the stimulation of mTOR-mediated protein synthesis as discussed above. In order to determine whether expression of the two genes is coupled, *Gl-Rheb* mRNA level was quantified in the same cDNA preparations used to quantify *Gl-Mstn* mRNA level (Covi et al., 2010). Interestingly, the relationship between *Gl-Rheb* and *Gl-Mstn* transcript levels differed in the two muscles. In thoracic muscle, *Gl-Rheb* log copy number was positively correlated with *Gl-Mstn* log copy number in both MLA and ESA animals (Fig. 9). In claw muscle, *Gl-Mstn* and *Gl-Rheb* mRNA levels were not correlated in MLA animals but were negatively correlated in ESA animals (Fig. 9). These data indicate that the regulation of *Gl-Rheb* by Mstn is complex and is not solely dependent on *Gl-Mstn* mRNA level. It is possible that *Gl-Rheb* expression is regulated by the level and/or activity of the Gl-Mstn mature protein. Proteolytic processing, secretion, proteolytic activation and inhibitory proteins (e.g. follistatin) can affect the activity of Mstn and other transforming growth factor-β (TGFβ) factors (reviewed by Breitbart et al., 2011; Moustakas and Heldin, 2009). Moreover, TGFβ signaling is downregulated by inhibitory Smad, protein phosphatases and ubiquitin-dependent degradation of TGFβ receptors and Smads (reviewed by Liu and Feng, 2010).

Autotomy-induced atrophy of the associated thoracic muscle segment also affects expression of mTOR signaling components. The unweighted thoracic muscle remains atrophied until a new limb is regenerated and 'weighting' is restored, along with full limb functionality (Moffett, 1987). This type of atrophy is akin to unloading atrophy in mammals (Jackman and Kandarian, 2004; Zhang et al., 2007). Unlike molt-induced atrophy, unweighting atrophy is not regulated by ecdysteroids, as this atrophy occurs during intermolt when ecdysteroid levels are low (Fig. 6E and Fig. 7E). *Gl-Mstn* mRNA level in unweighted thoracic muscle is 3-fold higher than in weighted muscle in intact animals but there is no difference in *Gl-Mstn* expression between weighted and unweighted muscles in premolt animals (Covi et al., 2010). By contrast, *Gl-Rheb* mRNA levels increased 2.2-fold in unweighted thoracic muscle in intact animals and remained elevated during premolt and post-molt (Fig. 10B). Contrary to expectations, reduced expression of *Gl-Rheb* or the other mTOR components (Fig. 10A) was not associated with higher levels of *Gl-Mstn* (Covi et al., 2010). In fact, *Gl-Rheb* and *Gl-Mstn* mRNA levels were positively correlated, emphasizing the differences between molt-induced atrophy and unweighting atrophy. The upregulation of *Gl-Rheb* and *Gl-s6k* suggests that unweighting stimulates global protein synthesis in thoracic muscle. This is an area for future study.

In summary, we have shown that *Gl-Rheb* is transcriptionally regulated by molting and unweighting in claw closer and thoracic muscles, respectively. Of the mTOR signaling genes, only *Gl-Rheb* mRNA levels were consistently increased in atrophic muscle. However, there were significant differences in how *Gl-Rheb* was regulated in the two muscles. *Gl-Rheb* expression in claw muscle appears to be stimulated by ecdysteroids, as *Gl-Rheb* mRNA level was correlated with hemolymph ecdysteroid level. This is consistent with our hypothesis that ecdysteroids stimulate mTOR-mediated protein synthesis. *Gl-Rheb* expression in thoracic muscle is not regulated by ecdysteroids, as there was no correlation between *Gl-Rheb* mRNA and ecdysteroid levels. The signal transduction pathway mediating the increased expression of *Gl-Rheb* in thoracic muscle in response to unweighting remains to be established. If *Gl-Mstn* plays a role in both types of atrophy, any unifying mechanism must reconcile the differences between *Gl-Mstn* and *Gl-Rheb* expression in the two muscles. In claw muscle, *Gl-Mstn* is downregulated when *Gl-Rheb* is upregulated whereas, in unweighted thoracic muscle, both *Gl-Mstn* and *Gl-Rheb* are upregulated. One possibility is that *Gl-Mstn* is a positive regulator of *Gl-Rheb* in thoracic muscle but is a neutral or negative regulator of *Gl-Rheb* in claw muscle. In shrimp (*Penaeus monodon*), RNAi knockdown of *Pm-Mstn* expression in abdominal muscle slows growth over a 45-day period (De Santis et al., 2011), suggesting that Mstn can stimulate muscle growth. Alternatively, regulation in thoracic muscle may instead be primarily post-transcriptional. The expression of *Gl-Mstn* and *Gl-Rheb* in both muscle types was not tightly coupled, indicating that transcriptional regulation of *Gl-Rheb* is complex and may differ between the claw and thoracic muscles in the relative contributions of ecdysteroid and Mstn regulation. In claw muscle, ecdysteroids may upregulate *Gl-Rheb* directly and *Gl-Mstn* may regulate other genes that inhibit the insulin/mTOR signaling pathway. For example, overexpression of Rheb-GAP inhibits mTOR activation and reduces fiber cross-sectional area in mammalian skeletal muscle (Wan et al., 2006). A further complication is that Mstn and its signaling through Smad transcription factors is regulated at multiple levels (e.g. Mstn processing, secretion and activation and modulation of Activin receptor and Smads) (Breitbart et al., 2011; Moustakas and Heldin, 2009) that could be affected by ecdysteroids. As transcription of *Gl-Rheb* in thoracic muscle does not involve ecdysteroids, Mstn/Smad or perhaps other signaling pathways have a greater role in regulating *Gl-Rheb* expression in unweighting atrophy. Now that key components of the insulin/mTOR and Mstn/Smad signaling pathways have been identified, future studies can be directed at gaining a mechanistic understanding of the interactions between ecdysteroids and the signaling pathways that control protein metabolism in crustacean skeletal muscle.

LIST OF ABBREVIATIONS

ESA	eyestalk ablation
EST	expressed sequence tag
GAP	GTPase-activating protein
Gl	*Gecarcinus lateralis*
MLA	multiple leg autotomy
Mstn	myostatin
mTOR	metazoan target of rapamycin
mTORC1	metazoan target of rapamycin Complex 1
ORF	open reading frame
qPCR	quantitative polymerase chain reaction
RACE	rapid amplification of cDNA ends
Rheb	Ras homolog enriched in brain
R-index	regeneration index
RT-PCR	reverse transcriptase-polymerase chain reaction
s6k	ribosomal S6 kinase
TGFβ	transforming growth factor-β
TOR	target of rapamycin
TSC	tuberous sclerosis complex

ACKNOWLEDGEMENTS

The authors thank Kira Marshall for assistance with tissue cDNA preparation for *G. lateralis* and *C. maenas*; Young Ji Kim and Sun Ok Lee for assistance with cloning the *Gl-Rheb* UTR sequences; Sharon A. Chang for measuring ecdysteroids by radioimmunoassay; Hector C. Horta for collecting *G. lateralis*; Staci Amburgey, Lisa Axtman, Peter Exner, Maddie Fountain, Jen Gunderson, Stefan LaBere, Kira Marshall, Katie Regelson, Ashanti Robinson and Sere Williams for animal care; and Christine M. Smith and David W. Towle, Mount Desert Island Biological Laboratory, for providing EST clones of lobster and green crab Rheb. We recognize the assistance of Ricardo Colon Alvarez (Executive Director, Consejo Dominicano de Pesca y Acuicultura, Dominican Republic) and his staff for expediting approval of permits, identifying suitable sites and collecting *G. lateralis*.

FUNDING

This study was funded by the National Science Foundation [NSF grant IOS-0618203].

REFERENCES

Abraham, R. T. and Wiederrecht, G. J. (1996). Immunopharmacology of rapamycin. *Ann. Rev. Immunol.* **14**, 483-510.

Agata, N., Sasai, N., Inoue-Miyazu, M., Kawakami, K., Hayakawa, K., Kobayashi, K. and Sokabe, M. (2009). Repetitive stratch suppresses denervation-induced atrophy of soleus muscle in rats. *Muscle Nerve* **39**, 456-462.

Amirouche, A., Durieux, A. C., Banzet, S., Koulmann, N., Bonnefoy, R., Mouret, C., Bigard, X., Peinnequin, A. and Freyssenet, D. (2009). Down-regulation of Akt/mammalian target of rapamycin signaling pathway in response to myostatin overexpression in skeletal muscle. *Endocrinol.* **150**, 286-294.

Aspuria, P. J. and Tamanoi, F. (2004). The Rheb family of GTP-binding proteins. *Cell. Signal.* **16**, 1105-1112.

Banzai, K., Ishizaka, N., Asahina, K., Suitoh, K., Izumi, S. and Ohira, T. (2011). Molecular cloning of a cDNA encoding insulin-like androgenic gland factor from the kuruma prawn *Marsupenaeus japonicus* and analysis of its expression. *Fish Sci.* **77**, 329-335.

Bengert, P. and Dandekar, T. (2003). A software tool-box for analysis of regulatory RNA elements. *Nucleic Acids Res.* **31**, 3441-3445.

Boyce, R., Chilana, P. and Rose, T. M. (2009). iCODEHOP: a new interactive program for designing COnsensus-DEgenerate Hybrid Oligonucleotide Primers from multiply aligned protein sequences. *Nucleic Acids Res.* **37**, W222-W228.

Breitbart, A., Auger-Messier, M., Molkentin, J. D. and Heineke, J. (2011). Myostatin from the heart: local and systemic actions in cardiac failure and muscle wasting. *Am. J. Physiol. Heart Circ. Physiol.* **300**, H1973-H1982.

Cardozo, C. P., Pan, J., Wu, Y., Bauman, W. A. and Qin, W. (2010). Anabolic steroids activate calcineurin-NFAT signaling in denervated muscle, and by this mechanism reduce denervation atrophy. *Endocrine Rev.* **31**, P2-4.

Castro, A. F., Rebhun, J. F., Clark, G. J. and Quilliam, L. A. (2003). Rheb binds tuberous sclerosis complex 2 (TSC2) and promotes S6 kinase activation in a rapamycin- and farnesylation-dependent manner. *J. Biol. Chem.* **278**, 32493-32496.

Chuang, N.-N. and Wang, P.-C. (1993). Characterization of phosphotyrosyl protein phosphatase from the hepatopancreas of the shrimp *Penaeus japonicus* (Crustacea: Decapoda). *J. Exp. Zool.* **266**, 181-187.

Chuang, N.-N. and Wang, P.-C. (1994). Characterization of insulin receptor from the muscle of the shrimp *Penaeus japonicus* (Crustacea: Decapoda). *Comp. Biochem. Physiol.* **108C**, 289-297.

Covi, J. A., Kim, H. W. and Mykles, D. L. (2008). Expression of alternatively spliced transcripts for a myostatin-like protein in the blackback land crab, *Gecarcinus lateralis*. *Comp. Biochem. Physiol.* **150A**, 423-430.

Covi, J. A., Bader, B. D., Chang, E. S. and Mykles, D. L. (2010). Molt cycle regulation of protein synthesis in skeletal muscle of the blackback land crab, *Gecarcinus lateralis*, and the differential expression of a myostatin-like factor during atrophy induced by molting or unweighting. *J. Exp. Biol.* **213**, 172-183.

De Santis, C., Wade, N. M., Jerry, D. R., Preston, N. P., Glencross, B. D. and Sellars, M. J. (2011). Growing backwards: an inverted role for the shrimp ortholog of vertebrate myostatin and GCF11. *J. Exp. Biol.* **214**, 2671-2677.

Drummond, M. J., Dreyer, H. C., Fry, C. S., Glynn, E. L. and Rasmussen, B. B. (2009a). Nutritional and contractile regulation of human skeletal muscle protein synthesis and mTORC1 signaling. *J. Appl. Physiol.* **106**, 1374-1384.

Drummond, M. J., Fry, C. S., Glynn, E. L., Dreyer, H. C., Dhanani, S., Timmerman, K. L., Volpi, E. and Rasmussen, B. B. (2009b). Rapamycin administration in humans blocks the contraction-induced increase in skeletal muscle protein synthesis. *J. Physiol.* **587**, 1535-1546.

Drummond, M. J., Miyazaki, M., Dreyer, H. C., Pennings, B., Dhanani, S., Volpi, E., Esser, K. A. and Rasmussen, B. B. (2009c). Expression of growth-related genes in young and older human skeletal muscle following an acute stimulation of protein synthesis. *J. Appl. Physiol.* **106**, 1403-1411.

Dunlop, E. A. and Tee, A. R. (2009). Mammalian target of rapamycin complex 1. Signalling inputs, substrates and feedback mechanisms. *Cell. Signal.* **21**, 827-835.

Dunlop, E. A., Dodd, K. M., Seymour, L. A. and Tee, A. R. (2009). Mammalian target of rapamycin complex 1-mediated phosphorylation of eukaryotic initiation factor 4E-binding protein 1 requires multiple protein–protein interactions for substrate recognition. *Cell. Signal.* **21**, 1073-1084.

El Haj, A. J. (1999). Regulation of muscle growth and sarcomeric protein gene expression over the intermolt cycle. *Am. Zool.* **39**, 570-579.

El Haj, A. J., Clarke, S. R., Harrison, P. and Chang, E. S. (1996). *In vivo* muscle protein synthesis rates in the American lobster *Homarus americanus* during the moult cycle and in response to 20-hydroxyecdysone. *J. Exp. Biol.* **199**, 579-585.

Fang, J. J. and Qiu, G. F. (2009). Molecular cloning of cyclin B transcript with an unusually long 3′ untranslation region and its expression analysis during oogenesis in the Chinese mitten crab, *Eriocheir sinensis*. *Molec. Biol. Rep.* **36**, 1521-1529.

Favier, F. B., Benoit, H. and Freyssenet, D. (2008). Cellular and molecular events controlling skeletal muscle mass in response to altered use. *Eur. J. Physiol.* **456**, 587-600.

Frost, R. A. and Lang, C. H. (2011). mTor signaling in skeletal muscle during sepsis and inflammation: where does it all go wrong? *Physiology* **26**, 83-96.

Furlow, J. D., Watson, M. L., Baehr, L. M., Karbassi, E., Reichardt, H. M., Tuckermann, J. P. and Bodine, S. C. (2010). The glucocorticoid receptor and its direct target gene MuRF1 are required for dexamethasone-induced skeletal muscle atrophy. *Endocrine Rev.* **31**, P1-39.

Gallardo, N., Carrillo, O., Molto, E., Deas, M., Gonzalez-Suarez, R., Carrascosa, J. M., Ros, M. and Andres, A. (2003). Isolation and biological characterization of a 6-kDa protein from hepatopancreas of lobster *Panulirus argus* with insulin-like effects. *Gen. Comp. Endocrinol.* **131**, 284-290.

Glass, D. J. (2010). Signaling pathways perturbing muscle mass. *Curr. Opinion Clin. Nutr. Metabol. Care* **13**, 225-229.

Griffis, B., Moffett, S. B. and Cooper, R. L. (2001). Muscle phenotype remains unaltered after limb autotomy and unloading. *J. Exp. Zool.* **289**, 10-22.

Gruber, A. R., Neuboeck, R., Hofacker, I. L. and Washietl, S. (2007). The RNAz web server: prediction of thermodynamically stable and evolutionarily conserved RNA structures. *Nucleic Acids Res.* **35**, W335-W338.

Hall, D. J., Grewal, S. S., de la Cruz, A. F. A. and Edgar, B. A. (2007). Rheb-TOR signaling promotes protein synthesis, but not glucose or amino acid import, in *Drosophila*. *BMC Biol.* **5**, 10.

Hatt, P. J., Liebon, C., Morinière, M., Oberlander, H. and Porcheron, P. (1997). Activity of insulin growth factors and shrimp neurosecretory organ extracts on a lepdopteran cell line. *Arch. Insect Biochem. Physiol.* **34**, 313-328.

Hietakangas, V. and Cohen, S. M. (2009). Regulation of tissue growth through nutrient sensing. *Ann. Rev. Genet.* **43**, 389-410.

Holland, C. A. and Skinner, D. M. (1976). Interactions between molting and regeneration in the land crab. *Biol. Bull.* **150**, 222-240.

Hu, X. L., Guo, H. H., He, Y., Wang, S. A., Zhang, L. L., Wang, S., Huang, X. T., Roy, S. W., Lu, W., Hu, J. J. et al. (2010). Molecular characterization of myostatin gene from zhikong scallop *Chlamys farreri* (Jones et Preston 1904). *Genes Genet. Syst.* **85**, 207-218.

Ismail, S. Z. M. and Mykles, D. L. (1992). Differential molt-induced atrophy in the dimorphic claws of male fiddler crabs, *Uca pugnax*. *J. Exp. Zool.* **263**, 18-31.

Jackman, R. W. and Kandarian, S. C. (2004). The molecular basis of skeletal muscle atrophy. *Am. J. Physiol.* **287**, C834-C843.

Kim, H. W., Mykles, D. L., Goetz, F. W. and Roberts, S. B. (2004). Characterization of a myostatin-like gene from the bay scallop, *Argopecten irradians*. *Biochim. Biophys. Acta* **1679**, 174-179.

Kim, H. W., Lee, S. G. and Mykles, D. L. (2005). Ecdysteroid-responsive genes, RXR and E75, in the tropical land crab, *Gecarcinus lateralis*: differential tissue expression of multiple RXR isoforms generated at three alternative splicing sites in the hinge and ligand-binding domains. *Mol. Cell. Endocrinol.* **242**, 80-95.

Kim, K.-S., Jeon, J.-M. and Kim, H.-W. (2009). A myostatin-like gene expressed highly in the muscle tissue of Chinese mitten crab, *Eriocheir sinensis*. *Fish Aqua. Sci.* **12**, 185-193.

Kim, K. S., Kim, Y. J., Jeon, J. M., Kang, Y. S., Oh, C. W. and Kim, H. W. (2010). Molecular characterization of myostatin-like genes expressed highly in the muscle tissue from Morotoge shrimp, *Pandalopsis japonica*. *Aquaculture Res.* **41**, e862-e871.

Kollias, H. D. and McDermott, J. C. (2008). Transforming growth factor-beta and myostatin signaling in skeletal muscle. *J. Appl. Physiol.* **104**, 579-587.

Kubica, N., Crispino, J. L., Gallagher, J. W., Kimball, S. R. and Jefferson, L. S. (2008). Activation of the mammalian target of rapamycin complex 1 is both necessary and sufficient to stimulate eukaryotic initiation factor 2B epsilon mRNA translation and protein synthesis. *Int. J. Biochem. Cell Biol.* **40**, 2522-2533.

Kucharski, L. C., Capp, E., Chittó, A. L. F., Trapp, M., Da Silva, R. S. M. and Marques, M. (1999). Insulin signaling: tyrosine kinase activity in the crab *Chasmagnathus granulata* gills. *J. Exp. Zool.* **283**, 91-94.

Kucharski, L. C., Schein, V., Capp, E. and da Silva, R. S. M. (2002). *In vitro* insulin stimulatory effect on glucose uptake and glycogen synthesis in the gills of the estuarine crab *Chasmagnathus granulata*. *Gen. Comp. Endocrinol.* **125**, 256-263.

Lai, E. C., Burks, C. and Posakony, J. W. (1998). The K box, a conserved 3′ UTR sequence motif, negatively regulates accumulation of enhancer of split complex transcripts. *Development* **125**, 4077-4088.

Lai, E. C., Roegiers, F., Qin, X. L., Jan, Y. N. and Rubin, G. M. (2005). The ubiquitin ligase *Drosophila* Mind bomb promotes Notch signaling by regulating the localization and activity of Serrate and Delta. *Development* **132**, 2319-2332.

Li, Y., Inoki, K. and Guan, K. L. (2004). Biochemical and functional characterizations of small GTPase Rheb and TSC2 GAP activity. *Mol. Cell. Biol.* **24**, 7965-7975.

Lin, C. L., Wang, P. C. and Chuang, N. N. (1993). Specific phosphorylation of membrane proteins of Mr 44,000 and Mr 32,000 by the autophosphorylated insulin receptor from the hepatopancreas of the shrimp *Penaeus monodon* (Crustacea, Decapoda). *J. Exp. Zool.* **267**, 113-119.

Lipina, C., Kendall, H., McPherron, A. C., Taylor, P. M. and Hundal, H. S. (2010). Mechanisms involved in the enhancement of mammalian target of rapamycin signalling and hypertrophy in skeletal muscle of myostatin-deficient mice. *FEBS Lett.* **584**, 2403-2408.

Liu, T. and Feng, X. H. (2010). Regulation of TGF-beta signalling by protein phosphatases. *Biochem. J.* **430**, 191-198.

Lo, P. C. H. and Frasch, M. (1999). Sequence and expression of myoglianin, a novel *Drosophila* gene of the TGF-β superfamily. *Mech. Dev.* **86**, 171-175.

Ma, D. Z., Bai, X. C., Guo, S. G. and Jiang, Y. (2008). The switch I region of Rheb is critical for its interaction with FKBP38. *J. Biol. Chem.* **283**, 25963-25970.

MacLea, K. S., Covi, J. A., Kim, H. W., Chao, E., Medler, S., Chang, E. S. and Mykles, D. L. (2010). Myostatin from the American lobster, *Homarus americanus*: cloning and effects of molting on expression in skeletal muscles. *Comp. Biochem. Physiol.* **157A**, 328-337.

Manning, B. D. and Cantley, L. C. (2003). Rheb fills a GAP between TSC and TOR. *Trends Biochem. Sci.* **28**, 573-576.

Manor, R., Weil, S., Oren, S., Glazer, L., Aflalo, E. D., Ventura, T., Chalifa-Caspi, V., Lapidot, M. and Sagi, A. (2007). Insulin and gender: an insulin-like gene expressed exclusively in the androgenic gland of the male crayfish. *Gen. Comp. Endocrinol.* **150**, 326-336.

Matsakas, A. and Patel, K. (2009a). Intracellular signalling pathways regulating the adaptation of skeletal muscle to exercise and nutritional changes. *Histol. Histopathol.* **24**, 209-222.

Matsakas, A. and Patel, K. (2009b). Skeletal muscle fibre plasticity in response to selected environmental and physiological stimuli. *Histol. Histopathol.* **24**, 611-629.

McCarthy, J. J. and Esser, K. A. (2010). Anabolic and catabolic pathways regulating skeletal muscle mass. *Curr. Opinion Clin. Nutr. Metabol. Care* **13**, 230-235.

McDonald, A. A., Chang, E. S. and Mykles, D. L. (2011). Cloning of a nitric oxide synthase from green shore crab, *Carcinus maenas*: a comparative study of the effects of eyestalk ablation on expression in the molting glands (Y-organs) of *C. maenas*, and blackback land crab, *Gecarcinus lateralis*. *Comp. Biochem. Physiol.* **158A**, 150-162.

Medler, S., Brown, K. J., Chang, E. S. and Mykles, D. L. (2005). Eyestalk ablation has little effect on actin and myosin heavy chain gene expression in adult lobster skeletal muscles. *Biol. Bull.* **208**, 127-137.

Mignone, F., Grillo, G., Licciulli, F., Iacono, M., Liuni, S., Kersey, P. J., Duarte, J., Saccone, C. and Pesole, G. (2005). UTRdb and UTRsite: a collection of sequences and regulatory motifs of the untranslated regions of eukaryotic mRNAs. *Nucleic Acids Res.* **33**, D141-D146.

Moffett, S. (1987). Muscles proximal to the fracture plane atrophy after limb autotomy in decapod crustaceans. *J. Exp. Zool.* **244**, 485-490.

Morissette, M. R., Cook, S. A., Buranasombati, C., Rosenberg, M. A. and Rosenzweig, A. (2009). Myostatin inhibits IGF-I-induced myotube hypertrophy through Akt. *Am. J. Physiol. Cell Physiol.* **297**, C1124-C1132.

Moustakas, A. and Heldin, C. H. (2009). The regulation of TGF beta signal transduction. *Development* **136**, 3699-3714.

Mykles, D. L. (1997). Crustacean muscle plasticity: molecular mechanisms determining mass and contractile properties. *Comp. Biochem. Physiol.* **117B**, 367-378.

Mykles, D. L. (1999). Proteolytic processes underlying molt-induced claw muscle atrophy in decapod crustaceans. *Am. Zool.* **39**, 541-551.

Mykles, D. L. (2001). Interactions between limb regeneration and molting in decapod crustaceans. *Am. Zool.* **41**, 399-406.

Mykles, D. L. (2011). Ecdysteroid metabolism in crustaceans. *J. Steroid Biochem. Mol. Biol.* **127**, 196-203.

Mykles, D. L. and Skinner, D. M. (1981). Preferential loss of thin filaments during molt-induced atrophy in crab claw muscle. *J. Ultrastruct. Res.* **75**, 314-325.

Mykles, D. L. and Skinner, D. M. (1982a). Crustacean muscles: atrophy and regeneration during molting. In *Basic Biology of Muscles: a Comparative Approach* (ed. B. M. Twarog, R. J. C. Levine and M. M. Dewey), pp. 337-357. New York: Raven Press.

Mykles, D. L. and Skinner, D. M. (1982b). Molt cycle-associated changes in calcium-dependent proteinase activity that degrades actin and myosin in crustacean muscle. *Dev. Biol.* **92**, 386-397.

Ohanna, M., Sobering, A. K., Lapointe, T., Lorenzo, L., Praud, C., Petroulakis, E., Sonenberg, N., Kelly, P. A., Sotiropoulos, A. and Pende, M. (2005). Atrophy of S6K1(–/–) skeletal muscle cells reveals distinct mTOR effectors for cell cycle and size control. *Nat. Cell Biol.* **7**, 286-294.

Otto, A. and Patel, K. (2010). Signalling and the control of skeletal muscle size. *Exp. Cell Res.* **316**, 3059-3066.

Patel, P. H., Thapar, N., Guo, L., Martinez, M., Maris, J., Gau, C. L., Lengyel, J. A. and Tamanoi, F. (2003). *Drosophila* Rheb GTPase is required for cell cycle progression and cell growth. *J. Cell Sci.* **116**, 3601-3610.

Proud, C. G. (2009). mTORC1 signalling and mRNA translation. *Biochem. Soc. Trans.* **37**, 227-231.

Reuther, G. W. and Der, C. J. (2000). The Ras branch of small GTPases: Ras family members don't fall far from the tree. *Curr. Opin. Cell Biol.* **12**, 157-165.

Rodgers, B. D. and Garikipati, D. K. (2008). Clinical, agricultural, and evolutionary biology of myostatin: a comparative review. *Endocrine Rev.* **29**, 513-534.

Rosen, O., Manor, R., Weil, S., Gafni, O., Linial, A., Aflalo, E. D., Ventura, T. and Sagi, A. (2010). A sexual shift induced by silencing of a single insulin-like gene in crayfish: ovarian upregulation and testicular degeneration. *PLoS ONE* **5**, e15281.

Schakman, O., Gilson, H., Kalista, S. and Thissen, J. P. (2009). Mechanisms of muscle atrophy induced by glucocorticoids. *Hormone Res.* **72**, 36-41.

Schmiege, D. L., Ridgway, R. L. and Moffett, S. B. (1992). Ultrastructure of autotomy-induced atrophy of muscles in the crab *Carcinus maenas*. *Can. J. Zool.* **70**, 841-851.

Shekhar, M. S. and Lu, Y. (2009). Application of nucleic-acid-based therapeutics for viral infections in shrimp aquaculture. *Mar. Biotechnol.* **11**, 1-9.

Skinner, D. M. (1962). The structure and metabolism of a crustacean integumentary tissue during a molt cycle. *Biol. Bull.* **123**, 635-647.

Skinner, D. M. (1965). Amino acid incorporation into protein during the molt cycle of the land crab, *Gecarcinus lateralis*. *J. Exp. Zool.* **160**, 225-234.

Skinner, D. M. (1968). Isolation and characterization of ribosomal ribonucleic acid from crustacean, *Gecarcinus lateralis*. *J. Exp. Zool.* **169**, 347-356.

Skinner, D. M. (1985). Molting and regeneration. In *The Biology of Crustacea* (ed. D. E. Bliss and L. H. Mantel), pp. 43-146. New York: Academic Press.

Skinner, D. M. and Graham, D. E. (1972). Loss of limbs as a stimulus to ecdysis in Brachyura (true crabs). *Biol. Bull.* **143**, 222-233.

Soulard, A., Cohen, A. and Hall, M. N. (2009). TOR signaling in invertebrates. *Curr. Opin. Cell Biol.* **21**, 825-836.

Sroyraya, M., Chotwiwatthanakun, C., Stewart, M. J., Soonklang, N., Kornthong, N., Phoungpetchara, I., Hanna, P. J. and Sobhon, P. (2010). Bilateral eyestalk ablation of the blue swimmer crab, *Portunus pelagicus*, produces hypertrophy of the androgenic gland and an increase of cells producing insulin-like androgenic gland hormone. *Tissue Cell* **42**, 293-300.

Stinckens, A., Georges, M. and Buys, N. (2011). Mutations in the myostatin gene leading to hypermuscularity in mammals: indications for a similar mechanism in fish? *Anim. Genet.* **42**, 229-234.

Su, J. S., Oanh, D. T. H., Lyons, R. E., Leeton, L., van Hulten, M. C. W., Tan, S. H., Song, L., Rajendran, K. V. and Walker, P. J. (2008). A key gene of the RNA interference pathway in the black tiger shrimp, *Penaeus monodon*: identification and functional characterisation of Dicer-1. *Fish Shellfish Immunol.* **24**, 223-233.

Teleman, A. A. (2010). Molecular mechanisms of metabolic regulation by insulin in *Drosophila*. *Biochem. J.* **425**, 13-26.

Thompson, J. D., Gibson, T. J., Plewniak, F., Jeanmougin, F. and Higgins, D. G. (1997). The CLUSTAL_X windows interface: flexible strategies for multiple sequence alignment aided by quality analysis tools. *Nucleic Acids Res.* **25**, 4876-4882.

Tisdale, M. J. (2009). Mechanisms of cancer cachexia. *Physiol. Rev.* **89**, 381-410.

Towle, D. W. and Smith, C. M. (2006). Gene discovery in *Carcinus maenas* and *Homarus americanus via* expressed sequence tags. *Integr. Comp. Biol.* **46**, 912-918.

Trendelenburg, A. U., Meyer, A., Rohner, D., Boyle, J., Hatakeyama, S. and Glass, D. J. (2009). Myostatin reduces Akt/TORC1/p70S6K signaling, inhibiting myoblast differentiation and myotube size. *Am. J. Physiol. Cell Physiol.* **296**, C1258-C1270.

Urso, M. L. (2009). Disuse atrophy of human skeletal muscle: cell signaling and potential interventions. *Med. Sci. Sports Exerc.* **41**, 1860-1868.

Ventura, T., Manor, R., Aflalo, E. D., Weil, S., Raviv, S., Glazer, L. and Sagi, A. (2009). Temporal silencing of an androgenic gland-specific insulin-like gene affecting phenotypical gender differences and spermatogenesis. *Endocrinol.* **150**, 1278-1286.

Wan, M., Wu, X. H., Guan, K. L., Han, M., Zhuang, Y. and Xu, T. (2006). Muscle atrophy in transgenic mice expressing a human TSC1 transgene. *FEBS Lett.* **580**, 5621-5627.

Wang, X. M., Fonseca, B. D., Tang, H., Liu, R., Elia, A., Clemens, M. J., Bommer, U. A. and Proud, C. G. (2008). Re-evaluating the roles of proposed modulators of mammalian target of rapamycin complex 1 (mTORC1) signaling. *J. Biol. Chem.* **283**, 30482-30492.

Welle, S., Bhatt, K., Pinkert, C. A., Tawil, R. and Thornton, C. A. (2007). Muscle growth after postdevelopmental myostatin gene knockout. *Am. J. Physiol. Endocrinol. Metab.* **292**, E985-E991.

Welle, S., Burgess, K. and Mehta, S. (2009). Stimulation of skeletal muscle myofibrillar protein synthesis, p70 S6 kinase phosphorylation, and ribosomal protein S6 phosphorylation by inhibition of myostatin in mature mice. *Am. J. Physiol. Endocrinol. Metab.* **296**, E567-E572.

Welle, S., Mehta, S. and Burgess, K. (2011). Effect of postdevelopmental myostatin depletion on myofibrillar protein metabolism. *Am. J. Physiol. Endocrinol. Metab.* **300**, E993-E1001.

Wennerberg, K., Rossman, K. L. and Der, C. J. (2005). The Ras superfamily at a glance. *J. Cell Sci.* **118**, 843-846.

Whiteley, N. M. and El Haj, A. J. (1997). Regulation of muscle gene expression over the moult in Crustacea. *Comp. Biochem. Physiol.* **117B**, 323-331.

Wu, Q. F., Law, P. Y., Wei, L. N. and Loh, H. H. (2008). Post-transcriptional regulation of mouse mu opioid receptor (MOR1) *via* its 3' untranslated region: a role for microRNA23b. *FASEB J.* **22**, 4085-4095.

Wullschleger, S., Loewith, R. and Hall, M. N. (2006). TOR signaling in growth and metabolism. *Cell* **124**, 471-484.

Yu, X. L., Chang, E. S. and Mykles, D. L. (2002). Characterization of limb autotomy factor-proecdysis (LAF_{pro}), isolated from limb regenerates, that suspends molting in the land crab *Gecarcinus lateralis*. *Biol. Bull.* **202**, 204-212.

Zeng, F., Xie, H., Nie, Z., Chen, J., Lv, Z., Chen, J., Wang, D., Liu, L., Yu, W., Sheng, Q. et al. (2009). Characterization of the gene *BmEm4*, a homologue of *Drosophila E(spl)m4*, from the silkworm, *Bombyx mori*. *Comp. Funct. Genom.* **209**, 947490.

Zhang, P., Chen, X. P. and Fan, M. (2007). Signaling mechanisms involved in disuse muscle atrophy. *Med. Hypotheses* **69**, 310-321.